JPRS-CST-87-015
9 APRIL 1987

China Report

SCIENCE AND TECHNOLOGY

FBIS FOREIGN BROADCAST INFORMATION SERVICE

JPRS-CST-87-015

9 APRIL 1987

China Report

SCIENCE AND TECHNOLOGY

FBIS FOREIGN BROADCAST INFORMATION SERVICE

105

NOTE

JPRS publications contain information primarily from foreign newspapers, periodicals and books, but also from news agency transmissions and broadcasts. Materials from foreign-language sources are translated; those from English-language sources are transcribed or reprinted, with the original phrasing and other characteristics retained.

Headlines, editorial reports, and material enclosed in brackets [] are supplied by JPRS. Processing indicators such as [Text] or [Excerpt] in the first line of each item, or following the last line of a brief, indicate how the original information was processed. Where no processing indicator is given, the information was summarized or extracted.

Unfamiliar names rendered phonetically or transliterated are enclosed in parentheses. Words or names preceded by a question mark and enclosed in parentheses were not clear in the original but have been supplied as appropriate in context. Other unattributed parenthetical notes within the body of an item originate with the source. Times within items are as given by source.

The contents of this publication in no way represent the policies, views or attitudes of the U.S. Government.

PROCUREMENT OF PUBLICATIONS

JPRS publications may be ordered from the National Technical Information Service, Springfield, Virginia 22161. In ordering, it is recommended that the JPRS number, title, date and author, if applicable, of publication be cited.

Current JPRS publications are announced in Government Reports Announcements issued semi-monthly by the National Technical Information Service, and are listed in the Monthly Catalog of U.S. Government Publications issued by the Superintendent of Documents, U.S. Government Printing Office, Washington, D.C. 20402.

Correspondence pertaining to matters other than procurement may be addressed to Joint Publications Research Service, 1000 North Glebe Road, Arlington, Virginia 22201.

JPRS-CST-87-015

9 APRIL 1987

CHINA REPORT

SCIENCE AND TECHNOLOGY

CONTENTS

ENVIRONMENTAL QUALITY

SCIENTISTS AND SCIENTIFIC ORGANIZATIONS

/9987

COMPANY MAPS OUT BLUEPRINT TO UPDATE TECHNOLOGY

Beijing CHINA DAILY: BUSINESS WEEKLY in English 11 Mar 87 p 1

[Article by Wang Xiangwei]

[Text]

Jilin Chemical Industrial Corporation, one of China's largest petro-chemical complexes, is trying every means to update its technology and machinery.

Located in Jilin, northeast China, the corporation is one of 156 major projects in China built with Soviet assistance in the 1950s and early 1960s.

A company official told Business Weekly that during the current five-year plan (1986-90) the company plans to invest a total of 930 million yuan on renovating Soviet-made machinery in order to lift most of its production lines to international standards.

Business Weekly learned the corporation has also been put on the list of 52 enterprises for which the State will invest about 20 billion yuan to improve in the next five years. Renovation of some of these industrial enterprises located in the Northeast has already started.

He said that the company will mainly rely on itself to update the machinery but it does not exclude the possibility of importing the Western technology to speed up the process.

"Since the Soviet Union has shown interest in updating the factories it helped built, we are also considering inviting them back as they are more familiar with our production system," the official said.

At present the corporation owns a dozen factories, manufacturing more than 200 varieties of petro-chemical products ranging from dyestuffs to acetaldehyde and employing about 50,000 workers.

But the corporation mainly built and developed itself three factories which produce dyestuffs, fertilizer, and calcium carbide, its three 'economic pillars.'

These factories, its the traditional profit makers, were built during the First Five-Year Plan (1953-57) under Soviet supervision and equipped with Soviet-made machinery.

Of the company's 88 major production facilities, 72 per cent were built in the 1950s and 15 per cent in the 1960s. This outdated machinery consumes large amounts of energy, unleashes pollutants, and turns out poor-quality products.

The fertilizer factory was the first to be built with the Soviet help. Construction began in 1954, and trial production in 1957. It was originally scheduled to be completed in three phases. But after the first was completed, the Soviet Union removed its experts following the deterioration in Sino-Soviet relations.

"So we had to finish the other two on our own," said Zan Zhuli, its general engineer. "And we encountered a lot of difficulties

because at that time we could neither turn to the Western countries nor to the Soviet Union for help."

They gathered as many foreign books on the relevant equipment needed as possible and tried to manufacture it themselves through numerous tests.

Finally they succeeded in completing the two phases, lifting the annual production volume of its major product, synthetic ammonia from 50,000 tons in the 1950s to the current 330,000 tons.

"The other two factories also went through similiar experiences," said an official from the general office of the corporation.

In 1978 and 1985, the company invited Japanese and American experts to its fertilizer factory to see whether they can help update the machinery but after the inspection the technicians concluded the machinery was too old-fashioned and suggested it should be scrapped and replaced.

Even Soviet experts said they could help renovate only some of the machinery because it no longer used machinery and technology like that transferred to the factory.

" Under such circumstances, we have to rely on ourselves to renovate those machinery as we cannot afford to replace the factory," said Zou.

The position is similiar with the other factories. So the company has established 9 research institutes to work on the development of new products and on the renovation, employing about 989 technical personnel.

This approach has paid off. Many scientific results have been rewarded by the State and turn out more profits when applied to production.

/9317
CSO: 4010/1017

LEASING FIRM PROMOTES WIDER USE OF COMPUTERS

Beijing CHINA DAILY: BUSINESS WEEKLY in English 11 Mar 87 p 3

[Article by Wang Yanping]

[Text]

Institutions and businesses lacking funds to computerize their units and foreign representative offices in China which want a leased computer now have someone to turn to — the China Computer Leasing Corporation which went into business last month in Beijing.

It leases different kind of computers, special facilities for offices, offers technical advice, training, and helps in installation, maintenance and programming.

"This is the first firm in our country to combine computer leasing and technical services," said Shang Zhicheng, vice president of the corporation. Our purpose is to promote the application of computers by reducing idle time of the expensive machines."

The leasing service comes in two forms. Customers who want eventually to own the leased computers may pay fees towards that purpose and the leasing corporation will transfer the ownership when the agreed amount is paid. Short term users just pay rent. During the leasing time, the corporation is responsible for the maintainance of the leased equipment.

After the establishment of the corporation, some representative offices of foreign companies in Beijing asked for microcomputers with Chinese processing functions.

"Foreign businessmen who held seminars or short-term training classes in China also want to rent computers from us," Shang Zhicheng said. And now the Great Wall 0520 CH, made in China and compatible with the IMB PC XT, is available.

The corporation also imports equipment from foreign countries according to customers requirements. If the customers are not able to pay foreign currency for the imported equipment, they may pay renminbi at a higher rate than the official one.

Two projects to computerize the banking systems in Shenyang of Liaoning Province and in Changzhou, Jiangsu Province, are being undertaken by the corporation, with a total value of about 50 million yuan.

The two cities' banking systems were selected by the State as experiments to set models for the nation's other banks and insurance companies.

The vice president said that some of the mainframe systems and terminals from abroad are expected to be installed by the end of this year.

China now has 41 leasing companies of various kinds, Sheng said, but his company is competitive because it has experienced backers and funds.

The strength comes mainly from China Leasing Corporation, one of its shareholders. It is one of the first leasing companies in China and has access to loans as its shareholders include China's four leading banks and the China International Trust and Investment Corporation.

The new corporation's other shareholder is China Computer Development Corporation which, under the Ministry of Electronics Industry, has experts and technicians in computer development and production.

This year's business volume is expected to reach about 70 million yuan compared with the planned target of 10 million yuan, Shang predicted.

/9317
CSO: 4010/1017

NON-STATE TECH FIRMS FLOURISH

Beijing CHINA DAILY in English 11 Feb 87 p 1

[Article by Dong Lisheng]

[Text] The appearance of nongovernmental technology development organizations "symbolizes great progress in the reform of the scientific and technological system" and will help establish a new mechanism for scientific research and production, Zeng Xianlin, Vice-Minister of the State Scientific and Technological Commission, said yesterday in Beijing.

The State attaches importance to such organizations "because we regard them as a way to bring into full play the scientists' and technicians' initiative," Zeng told a forum for nongovernmental technology development organizers.

According to Chen Shengwu, a member of the Secretariat of the Chinese Scientific and Technical Association, since the first group of such organizations emerged in the early 1980s their number has multiplied to about 10,000, with more than 200,000 employees.

Compared with government-funded research institutions, said Chen, they are more flexible in operation and management and more directly serve the market and their users. With sole responsibility for profits and losses, they offer a complete range of services including research and development, production, sales and maintenance, he said.

The organizations are formed by individual technicians and scientists or by collective units on a voluntary basis. Most of them are making a profit.

For instance, Chen said, a recent survey showed that 141 such institutions in the Haidian District in northwest Beijing undertook more than 3,700 development projects from January 1984 to March 1986, 200 of them new in China. These projects had a combined value of 170 million yuan (about $45.9 million), and turned over to the State 58 million yuan ($15.6 million) in taxes. They also donated 500,000 yuan ($135,000) to public projects.

The four-day forum aims to sum up the experiences of those running such organizations and to appeal the relevant government departments to create protective policies and offer them more favourable treatment in taxes and loans, Chen said.

Zeng stressed that the experiences of the forum participants proved the urgency of getting rid of old ideas.

The old management system must be broken and the concept of equal competition between research institutions established, Zeng said. The practice of bidding for research projects should be adopted, and poorly-operated institutions could be leased out, he said.

And, Zeng added, "We should allow scientists and technicians who help others become rich also improve their own livelihoods"

/12828
CSO: 4010/2012

CHINA PREPARES TO LAUNCH FIRST CANCER PROGRAM

Beijing CHINA DAILY in English 10 Mar 87 p 1

[Article by Wen Jia]

[Text]

For the first time since the founding of the People's Republic, China is drawing up its national programme to combat cancer — a disease which is said to claim 17 lives every 10 minutes in this country.

The programme, to extend till the end of the century, is aimed at reducing the incidence of cancer, cutting the death rate and improving patients' lives in the later stages of the disease. It is expected to be launched later this year.

Experts believe cancer now is the No. 1 killer of Chinese aged between 20 and 59, a group representing about 40 per cent of the population. It ranks the third — next only to heart trouble and cerebrovascular disease — for all mainland Chinese.

Chen Miaolan, head of the Cancer Control Agency under the Ministry of Public Health, told China Daily over the weekend that the programme would include setting up a three-tier network for cancer prevention and treatment. "Efforts will be made in all walks of society to fight cancer," Chen said.

"We'll try to co-ordinate with other organizations to improve people's living and working conditions and dissuade them from smoking, drinking excessively and eating too many pickled and smoked foods," she said.

But first, offices of cancer control will be opened or strengthened in the 29 provinces, municipalities and autonomous regions of the Chinese mainland, especially in high-incidence areas.

More cancer hospitals and sections specializing in cancer prevention in ordinary hospitals will be added to the present 26 cancer hospitals and institutions in the country, which fall far short of needs. And more medical personnel will be trained.

A national data bank will be built in Beijing to monitor cases and the death rate, and facilities for cancer prevention and treatment will be improved across the country.

Chen said that they would concentrate on the early discovery, diagnosis and treatment of cancer patients, which are the keys to saving or prolonging lives.

Under the Seventh Five-year Plan, China will see 37 research projects completed on the prevention and treatment of cancer, according to Li Liandi, director of the office of national cancer control.

China is thought to have 900,000 deaths from cancer a year now, compared to 700,000 in the mid-1970s, when the country conducted its first national medical survey.

The past 10 years have seen little change in the death rates from stomach, esophagus and liver cancer but there have been increases in cancer of the lung, intestines and breast, Li said.

China has achieved much in cancer research in the past years and is approaching or exceeding the world's advanced levels in treatment, Chen Miaolan said. But the country is still poor in its prevention work and facilities for treatment, especially in the countryside and remote areas, she added.

In Shanghai, where facilities for cancer control are among the best in China, only 1 to 3 per cent of liver, lung and esophagus cancer cases and 4 to 6 per cent of stomach and intestinal cancer cases were diagnosed at their early stages in early 1985, according to the city's medical statistics.

Chen attributed the low rate of early diagnosis to the shortage of cancer hospitals and the unpopularity of effective methods in the cancer divisions of ordinary hospitals, where about 90 per cent of cancer patients are treated.

"We are now spending a large part of our limited funds on more and better experimental units in high-incidence areas and on spreading advanced experiences and techniques," Chen said.

"We are also open to the achievements in cancer treatment in other parts of the world,"she said.

/9317
CSO: 4010/1017

BENDING MAGNET FOR ELECTRON-POSITRON COLLIDING MACHINE

Beijing CHINA MACHINERY in English 25 Sep 86 pp 15

[Summary] The manufacture of the curve-tined magnet used in the main storage ring of the electron-positron colliding machine, which was undertaken by Xianfeng Electric Machinery Factory in Shanghai was completed on September 29 this year. After the inspection of the magnet Madame Wu Jianxiong and Mr. Yuan Jialiu, the famous physicists from USA, remarked that 'the magnet you made is even better than those made in USA'. The electron-positron colliding machine in Beijing is rated as a key state construction project. And the curve-tined magnet of the storage ring is one of the eight most important pieces of equipment. The magnet consists of 42 sectors, each weighing 8 tons. Its function is to generate high precision magnetic field to ensure that electrons and positrons move along a controllable orbit so as to guarantee the collision. The magnetic field must be highly homogeneous and the machining precise, and hence very difficult to manufacture.

/12828
CSO: 4010/2012

MINIMUM OIL CIRCUIT BREAKER

Beijing CHINA MACHINERY in English 25 Sep 86 p 18

[Summary] The Shenyang HV Switchgear Factory recently developed and manufactured a HV minimum-oil circuit breaker of 220 KV, the biggest one in the country. The circuit breaker passed technical appraisal by the Ministry of Machine Building Industry and the Ministry of Water Resources & Electric Power on 9 September in Beijing. Relevant experts consider that the success of manufacturing such a product is an important breakthrough in the field of high voltage switch manufacture in our country.

Model SWZ-220 minimum-oil circuit breaker produced by Shenyang HV Switchgear Factory was the first one whose current reached 31.5 KA in 1980. Then, it undertook to switch a long loadless circuit of 369 Km in the northeast grid. In the past few years, factory personnel made technical analysis to the structure and characteristics of their product and they believe that it is impossible to increase its capacity. In 1984, they started to improve the capacity of the breaker. In 2 years they made more than ten important modifications and made tests strictly on the international standard 6,500 times. Finally, the rated current of 31.5 KA increased to 40 KA and met IEC Standard. Examined and inspected by more than 30 experts, the circuit breaker, capable of switching current up to 40 V, is an important breakthrough in the history of high voltage minimum-oil breaker manufacturing in our country.

/12828
CSO: 4010/2012

FIRST INSTRUMENT FOR DIAGNOSING FAULTS

Beijing CHINA MACHINERY in English 25 Sep 86 p 20

[Summary] Model ED5900 pocket instrument for diagnosing faults for mechanical equipment, the first in China, trial-produced by Tianjin No. 2 Electronic Instrument Factory has passed the appraisal. The experts believed that this instrument fills in the gap in the fault diagnostic technology for mechanical equipment in China. The new technology has been developed in recent years. At present, measuring methods are very backward. Using the new instrument, displacement, speed and acceleration of machine vibration, whose frequency is below 4000 Hz and above 10 Hz, can be measured. The results are shown by liquid crystal display. After compared with normal data, the machine's working conditions can be known and the wrong places can also be found. After using the instrument, Wuhan Iron & Steel Complex and Tianjin Textile Machinery Plant stated that the instrument works fast, accurately and is easy to operate. It weighs 450 g and no more than 1 Kg connected with transducer. It only needs 45 batteries to work and it is easy to carry.

/12828
CSO; 4010/2012

NEW WELDING RODS

Beijing CHINA MACHINERY in English 25 Sep 86 p 20

[Summary] JH-J506DC welding rods, a new welding material, co-developed by Jinzhou Welding Rods Factory and Harbin Welding Research Institute, passed appraisal on August 26. As a key state scientific and technical project, the welding rod research task was given by the State Economic Commission in 1984. It took two years to design and produce. The performance testing shows that the main properties of J506DC are better than LB-52Y made in Japan, and reaches advanced international level. There is a great need for this rod in ocean projects, ship-building and offshore oil extraction.

/12828
CSO: 4010/2012

SUPERCONDUCTING CURRENT COMPARATOR

Beijing CHINA MACHINERY in English 25 Nov 86 p 21

[Article by Lu Jingsan]

[Text] Superconducting current comparator is used for measurement of resistance, temperature coefficient of resistance, load factor and ratio of the two resistances. It is also used for measuring current, voltage and quantity of non-electricity converted to quantity of electricity and their ratio; physical constant of 2e/h (h — Plank constant and e — electronic charge); it can be used as an electric resistance thermometer or a key device for Jafferson voltage reference.

Superconducting current comparator is a fruit of international development in 1970s and used in measurement labs in the developed countries. The China National Metrological Research Institute first in China developed such comparators of novel design. These comparators are three orders of magnitude higher than the conventional instruments in terms of their technical parameters. The comparators have reached the international advanced level in terms of the noise level and ratio error. In these respects they are superior to the standards applied in Australia, U.K., France, Italy and Finland.

The comparator has recently passed the appraisal and has opened up new vistas for the manufacture in China of high sensitivity measuring instruments.

/12828
CSO: 4010/2012

PLANTS EMPLOY NEW ORE EXTRACTION TECHNIQUE

OW131322 Beijing XINHUA in English 1232 GMT 13 Mar 87

[Text] Beijing, 13 Mar (XINHUA)--Last year two ore dressing plants affiliated with China's Capital Iron and Steel Company showed profits of 20 million yuan (U.S.$5.4 million).

The company attributed the success to a new magnetic-agglomeration gravity separation technique introduced at the beginning of 1986.

An official of the Science and Technology Department of China's Ministry of Geology and Mineral Resources told XINUUA today, "The new technique separates valuable ore from waste products using magnets."

"This separation technique is a new invention and important breakthrough in China in the extraction of magnetic ore," the official said.

"In the past, China has stuck to traditional methods of processing ore," he added, "but these methods were inefficient and sometimes unable to separate adequately valuable minerals effectively."

"One ore dressing can still process 6.5 million tons of ore annually," the official said, "but the amount of high-grade ore recovered has increased by 16 percent."

The Anshan Iron and Steel Company, China's largest, and other major related companies nationwide will soon adopt this new technique in their operations.

Study on the new technology began in 1978, and was finally improved by the Institute of Mineral Resource Utilization in 1986. The work was done with the cooperation of the Ministry of Geology and Mineral Resources, the Zhengzhou Institute of Mineral Resource Utilization and the Capital Iron and Steel Company.

In 1986, the invention earned a gold medal from China's Association of Inventions.

/6662
CSO: 4010/2011

BRIEFS

S&T REFRESHER COURSES--Wuhan, 9 Mar (XINHUA)--Refresher courses have helped scientists and technicians in Hubei Province broaden and enrich their professional knowledge in the past two years. More than 80,000 technicians in the province have attended on-the-job training courses, according to an official of the provincial scientific and technological personnel bureau. Huangshi conducted 105 courses last year with a combined enrollment of 5,200 students, accounting for 12.8 of the total technicians in the city. Most trainees completed their schooling in the 1950s and early 1960s. They are the backbone of many key research units and enterprises, but their knowledge has become outdated with new developments in science and technology. China's modernization requires them to refresh their knowledge and master the most advanced technology in the world. [Text] [Beijing XINHUA in English 0907 GMT 9 Mar 87 OW]/6662

HEBEI SPARK PLAN--Shijiazhuang, 5 Feb (XINHUA)--China's "spark plan" has helped Hebei Province earn 490 million yuan (US$132 million) last year. In addition to 20,000 staff members from provincial research institutes, Hebei invited 300 experts from outside the province to assist in rural enterprises and mountainous areas. Under the plan, in 1986 the provincial science and technology commission helped train 26,000 farmers, and provided up-to-date farming technology and information to two-thirds of the province's cities and countries. The commission has also raised nine million yuan (US$2.4 million) to fund projects under the plan. [Summary] [Beijing XINHUA in English 1431 GMT 5 Feb 87 OW] /6662

ZHOU GUANGZHOU STRESSES BASIC RESEARCH--Beijing, 15 Mar (XINHUA)--President Zhou Guangzhou of the Chinese Academy of Sciences [CAS] said here today that the CAS will give scope to its advantages and attach importance to basic research. Speaking at a working conference of the CAS, which closed here today, he added that those technology-related institutes should also pay attention to basic research. He noted that most of the CAS's products that have entered the international market come from the research institutes engaged in basic research. While efforts are being made to work for the national economy, no institute is allowed to abandon basic research, he said. He criticized the reluctance to spend money on basic research projects during technical cooperation and described this as short-sighted. Zhou also said that democracy should be displayed fully in defining the direction of research work and selecting research topics. Sensory appeal and imagination of individual scientists are very important during the exploration period and, therefore, a certain

proportion of research topics for self-selection should be reserved for scientists, so as to help create an environment for their independent thinking and exploring. [Summary] [Beijing XINHUA in English 1224 GMT 15 Mar 87 OW] /6662

MANAGEMENT SCIENCE FOUNDATION--Beijing, 11 Mar (XINHUA)--China has set up a business management science foundation to fund research into business management science, the State Economic Commission announced here today. The foundation, inaugurated March 7, is chaired by Yuan Baohua, president of the Chinese Enterprise Management Association and president of the Chinese People's University in Beijing. The foundation will accept donations from foreign governments, international organizations, enterprises, and nongovernmental organizations and individuals, as well as from Chinese enterprises, people's organizations, collectives and individuals. A nonprofit organization approved by the State Economic Commission and the People's Bank of China, the foundation will encourage enterprises and academic institutions to foster scientific management. [Text] [Beijing XINHUA in English 1449 GMT 11 Mar 87 OW] /6662

CSO: 4010/2011

PHYSICAL SCIENCES

IMPROVEMENT OF CHEN'S THEOREM

Shanghai ZIRAN ZAZHI [NATURE JOURNAL] in Chinese Vol 9, No 10, Oct 86 p 794

[Article by Wu Donghua [6762 0392 5478]; paper received 23 Sep 85]

[Text] In this paper, let x be a sufficiently large even number, let h be any even number, $C_{xq}=\prod_{p|xq}\frac{p-1}{p-2}\prod_{p>2}\left(1-\frac{1}{(p-1)^2}\right)$;

Also, let $P_x(1,1)$ be the number of prime numbers that satisfy the following condition: $x - p = p_1$, where p_1 is a prime number. Let $x_h(1,1)$ be the number of prime numbers that satisfy the following condition: $p \leq x$, $p+h = p_1$. It has been shown in References [1,2] that

$$\begin{aligned} P_x(1,1) &\leqslant \frac{16xC_x}{(\log x)^2}, \\ x_h(1,1) &\leqslant \frac{16xC_x}{(\log x)^2}. \end{aligned} \tag{1}$$

In 1956, Wang Yuan[3] proved under the generalized Riemann assumption that the coefficient "16" in equation (1) can be replaced by "8". In 1964, Pang Chengdong[4] proved that "16" can be replaced by "12". In 1966, Bombieri and Davenport[5] further improved this number to be "8". In 1978, Chen Jingren[6] proved that the coefficient in equation (1) can be taken as 7.8342. We have proved the following Theorem for a sufficiently large even number x, we have

$$P_x(1,1) \leqslant \frac{7.81565\,x\,C_x}{(\log x)^2}.$$

REFERENCES

[1] Чулановский И. В., *ДАН СССР*, **63** (1948) 491

[2] Selberg A., 11 *Skand. Mat. Kongr.*, Trondhjem (1949) 13

[3] Wang Yuan, "Acta Matematica Sinica", 6 (1956), p 565; "Acta Mathematica Sinica", 10 (1960), p 161; Sci. Sin., 11 (1962) p 1033.

[4] Pang Chengdong, "Acta Matematica Sinica", 14 (1964) p 597; Sci. Sin., 13 (1964) p 1045.

[5] Bombieri E., Davenport H., *Proc. Roy. Soc.*, Ser. A, **293** (1966) 1

[6] Chen Jingren, Sci. Sin., 21 (1978) p 701.

(Received 23 September 1985)

3012/7358
CSO: 4008/1027

PHYSICAL SCIENCES

PROBABILISTIC INNER PRODUCT SPACES

Chongqing YINGYONG SHUXUE HE LIXUE [APPLIED MATHEMATICS AND MECHANICS] in Chinese Vol 7, No 11, Nov 86 pp 976-981

[Article by Zhang Shisheng [1728 4258 3932]]

[Text] I. Introduction

The theoretical and applied research of probabilistic metric spaces and probabilistic normed spaces is a new important topic in the study of random functional analysis. With the development of this theory, the concept of probabilistic inner product space has recently been introduced in References [1,3,4], and certain related theories have been established. But a key problem that still remains unsolved is to agree on a rational and comprehensive definition of probabilistic inner product spaces.

In this paper, an attempt is made to solve the above problem. In section 2 of this paper we give a new definition of probabilistic inner product space, and show that the conventional inner product space is a special case of this definition. To demonstrate the rationality of this definition, a comparison with conventional inner product space is given in section 3. In sections 4 through 6, we establish the Schwarz inequality and the concept of orthogonality of probabilistic space and discuss its relationship with probabilistic normed space.

II. Definition and Examples of Probabilistic Inner Product Spaces

In this paper, the following notations shall be used: $R=(-\infty,\infty)$, $R^+=[0,\infty)$; $\mathscr{D}$ denotes the set of all left-continuous distribution functions; $\mathscr{D}^+=\{F\in\mathscr{D}:\ F(0)=0\}$.

Also, let

$$H(t)\doteq\begin{cases}1 & (t>0)\\ 0 & (t\leqslant 0)\end{cases}$$

Function Δ: $[0,1]\times[0,1]\to[0,1]$ is called a t-norm, if for all a, b, c, $d\in[0,1]$, the following conditions are satisfied:

$(\Delta\text{-}1)\quad \Delta(a,1)=a;$

$(\Delta\text{-}2)\quad \Delta(a,b)=\Delta(b,a);$

$(\Delta\text{-}3)$ when $c\geqslant a, d\geqslant b$时, $\Delta(c,d)\geqslant\Delta(a,b);$

$(\Delta\text{-}4)\quad \Delta(a,\Delta(b,c))=\Delta(\Delta(a,b),c).$

We call the t-norm $\Delta_1 \geqslant \Delta_2$ if $\Delta_1(a,b)\geqslant\Delta_2(a,b)$, $\forall a,b\in[0,1]$. We shall use the notation Δ_m to denote a special t-norm defined by:

$$\Delta_m(a,b)=\max\{a+b-1,0\}\qquad (\forall a,b\in[0,1])$$

Definition 1. The three element group $(E,\mathcal{F},\Delta)$ is called a probabilistic inner product space if E is a real linear space, Δ is a t-norm, and $\mathcal{F}$ is a $E\times E\to\mathcal{D}$ mapping which satisfies the following conditions (in what follows, we shall use the notation $\mathcal{F}(x,y)=F_{x,y}$, and $F_{x,y}(t)$ represents the value of $F_{x,y}$ for $t\in R$):

$$(\text{PI-1})\qquad F_{x,x}(0)=0;$$

$$(\text{PI-2})\qquad F_{x,y}=F_{y,x};$$

$$(\text{PI-3})\qquad F_{x,x}(t)=H(t),\ \forall t\in R\Leftrightarrow x=\theta;$$

$$(\text{PI-4})\qquad F_{\alpha x,y}(t)=\begin{cases}F_{x,y}\left(\frac{t}{\alpha}\right) & (\alpha>0)\\ H(t) & (\alpha=0)\\ 1-F_{x,y}\left(\frac{t}{\alpha}+\right) & (\alpha<0)\end{cases}$$

where α is any real number, and $F_{x,y})t/\alpha+)$ represents the right limit of $F_{x,y}$ at t/α;

$$(\text{PI-5})\qquad F_{x+y,z}(t)=\sup_{\substack{s+r=t\\ s,r\in R}}\Delta(F_{x,z}(s),F_{y,z}(r))\qquad (t\in R).$$

Example: let E be a real inner product space, and let us define the mapping $\mathcal{F}$: $E\times E\to\mathcal{D}$ as follows:

$$F_{x,y}(t)=H(t-(x,y))\tag{2.1}$$

We shall now prove that $(E,\mathcal{F},\Delta)$ is a probabilistic inner space, where Δ is a t-norm.

In fact, conditions (PI-1) ~ (PI-3) are obviously satisfied. Also, for any $\alpha\in R$, when $\alpha>0$, we have

$$F_{\alpha x,y}(t)=H(\alpha(t/\alpha-(x,y))=H(t/\alpha-(x,y))=F_{x,y}(t/\alpha)$$

when $\alpha=0$, $F_{x,y}(t)=H(t)$; when $\alpha<0$, we have

$$F_{\alpha x,y}(t)=H\left(-\alpha\left(-\frac{t}{\alpha}+(x,y)\right)\right)=H\left(-\frac{t}{\alpha}+(x,y)\right)=1-F_{x,y}\left(\frac{t}{\alpha}+\right)$$

hence condition (PI-4) is established.

When $t>(x+y,z)$, for any t_1, $t_2 \varepsilon R$, $t_1+t_2=t$, and $t_1>(x,z)$, $t_2>(y,z)$. Therefore,

$$1=H(t-(x+y,z))=F_{x+y,z}(t)=\Delta(H(t_1-(x,z)),\ H(t_2-(y,z)))$$
$$=\sup_{\substack{s+r=t\\ s,r\in R}} \Delta(F_{x,z}(s),F_{y,z}(r))$$

When $t \leqslant (x+y,z)$, for any s, $r \varepsilon R$, $s+r=t$, regardless whether $s>(x,z)$ (hence $r<(y,z)$) or $s<(x,z)$, we have:

$$F_{x+y,z}(t)=H(t-(x+y,z))=0=\sup_{\substack{s+r=r\\ s,r\in R}} \Delta(H(s-(x,z)),\ H(r-(y,z)))$$

hence condition (PI-5) is established. Thus, proof is complete.

III. Comments and Comparisons

Let $(E,\mathscr{F},\Delta)$ be a probabilistic inner product space. Let $\mathscr{E}$ be an interval on $\mathscr{F}$, i.e.,

$$\mathscr{E}=\{F_{x,y}\in\mathscr{D}:\ x,y\in E\}$$

For any fixed $z\varepsilon E$, let

$$\mathscr{E}_z=\{F_{x,z}\in\mathscr{D}:\ x\in E\}$$

Now we introduce the following addition and multiplication operations for the elements in $\mathscr{E}_z$:

$$\alpha\circ F_{x,z}=F_{\alpha x,z},\quad F_{x,y}\oplus F_{y,z}=F_{x+y,z} \tag{3.1}$$

Then the following result is obtained.

Proposition 1

Let $(E,\mathscr{F},\Delta)$ be a probabilistic inner product space with continuous t-norm Δ. Then the set $\mathscr{E}_z$ constitutes a linear space based on the operations given in (3.1), and $\mathscr{E}_z$ is the homomorphic mapping of E.

Proof

It follows from the definition of probabilistic inner product space that $\mathscr{E}_z$ is closed with respect to the operations of (3.1);

furthermore, we have:

(i) $F_{x,z} \oplus F_{y,z} = F_{y,z} \oplus F_{x,z}$;

(ii) $(F_{x,z} \oplus F_{y,z}) \oplus F_{u,z} = F_{x,z} \oplus (F_{y,z} \oplus F_{u,z})$;

(iii) has zero element $F_{\theta,z}=H$, and

$$F_{x,z} \oplus F_{\theta,z} = F_{\theta,z} \oplus F_{x,z} = F_{x,z};$$

(iv) for each element $F_{x,z} \varepsilon \mathcal{E}_z$, there is an inverse element $F_{-x,z} \varepsilon \mathcal{E}_z$ such that $F_{x,z} \oplus F_{-x,z} = H$.

(v) $(\alpha\beta) \circ F_{x,z} = \alpha \circ (\beta \circ F_{x,z})$;

(vi) $\alpha \circ (F_{x,z} \oplus F_{y,z}) = \alpha \circ F_{x,z} \oplus \alpha \circ F_{y,z}$;

(vii) $(\alpha+\beta) \circ F_{x,z} = \alpha \circ F_{x,z} \oplus \beta \circ F_{x,z}$;

(viii) $1 \circ F_{x,z} = F_{x,z}$;

(ix) $0 \circ F_{x,z} = H$.

Thus, we have proved that $\mathcal{E}_z$, $z \varepsilon E$ is a linear space. Let

$$\psi: x \mapsto F_{x,z}$$

it can be readily shown that for any $\alpha, \beta \varepsilon R$, $x, y \varepsilon E$, we have:

$$\psi(\alpha x + \beta y) = \alpha \circ \psi(x) \oplus \beta \circ \psi(y)$$

Therefore, $\mathcal{E}_z$, $z \varepsilon E$ is the homomorphic mapping of E. Thus, proof of the proposition is complete.

Now we introduce the partial order "$\leq$" in the following sense: if F, $G \varepsilon \mathcal{E}$, then $F \leq G$ if and only if $F(t) \geq G(t)$, $\forall t \varepsilon R$. If we write

$$\langle x,y \rangle = F_{x,y} \qquad (x,y \in E)$$

then from the conditions (PI-1) ~ (PI-5) and proposition 1, we have:

(i) $\langle x,y \rangle = \langle y,x \rangle \quad (\forall x,y \in E)$;

(ii) $\langle x,x \rangle \geqslant H$, 又 $\langle x,x \rangle = H \Leftrightarrow x=\theta$.

(iii) $\langle \alpha x, y \rangle = \alpha \circ \langle x,y \rangle$;

(iv) $\langle x+y, z \rangle = \langle x,z \rangle \oplus \langle y,z \rangle$.

therefore, the definition of probabilistic inner product space introduced here is consistent with the definition of conventional inner products.

IV. Schwarz Inequality of Probabilistic Inner Product Space

Theorem 1

Let $(E, \mathcal{F}, \Delta)$ be a probabilistic inner product space, and let Δ satisfy the condition: $\Delta(t,t) \geq t$, $\forall t \varepsilon [0,1]$. Then for any $u, v, \varepsilon E$ and any $t > 0$, $s > 0$, we have:

$$F_{u,v}(ts+) \geqslant \Delta(F_{u,u}(t^2),\ F_{v,v}(s^2)) \tag{4.1}$$

((4.1) will be referred to as Schwarz inequality of the probabilistic inner product space).

Proof

Let $\alpha=-s/t$, hence $\alpha t + s=0$. Let $a=F_{u,u}(s^2)$, $b=F_{av,u}(ats)$, $c=F_{av,av}(\alpha^2t^2)$.

Then from conditions (PI-1) and (PI-5), we have:

$$\begin{aligned} 0&=F_{u+av,u+av}((\alpha t+s)^2) \geqslant \Delta(\Delta(a,b),\ \Delta(b,c)) \\ &=\Delta(a,\Delta(\Delta(b,b);c)) \geqslant \Delta(a,\Delta(b,c)) \end{aligned} \tag{4.2}$$

Also, from $\Delta(t,t) \geqslant t$, $\forall t \varepsilon [0,1]$, it follows that $\Delta \geqslant \Delta_m$. Furthermore,

$$c=F_{av,av}(\alpha^2t^2)=1-F_{v,av}(\alpha t^2+)=F_{v,v}(t^2)$$
$$b=F_{av,u}(\alpha ts)=1-F_{v,u}(ts+)$$

Therefore, from (4.2), we obtain:

$$\begin{aligned} &0 \geqslant \Delta(F_{u,u}(s^2),\ \Delta(1-F_{v,u}(ts+),F_{v,v}(t^2))) \\ &=\Delta(\Delta(F_{u,u}(s^2),\ F_{v,v}(t^2)),\ 1-F_{v,u}(ts+)) \\ &(\text{因}\Delta \geqslant \Delta_m) \geqslant \Delta(F_{u,u}(s^2),\ F_{v,v}(t^2))+1-F_{v,u}(ts+)-1 \end{aligned}$$

hence $$F_{u,v}(ts+) \geqslant \Delta(F_{u,u}(s^2),\ F_{v,v}(t^2))$$

Q.E.D.

V. Menger Probabilistic Inner Product Space and Its Topology

Definition 2

Let $(E,\mathcal{F},\Delta)$ be a probabilistic inner product space where Δ is a continuous t-norm which satisfies the condition $\Delta(t,t) \geqslant t$, $\forall t \varepsilon [0,1]$. Also, assume that for any $t>0$, $s>0$, the following inequality holds:

$$F_{u,v}(ts) \geqslant \Delta(F_{u,u}(t^2),\ F_{v,v}(s^2)) \qquad (\forall u,v \in E) \tag{5.1}$$

then $(E,\mathcal{F},\Delta)$ is called a Menger probabilistic inner product space.

Definition 3

(E,f,Δ) is called a probabilistic normed space if E is real linear space, Δ is a t-norm, f is a $E \to \mathcal{D}$ mapping (we shall use the notation $f(x)=f_x$) which satisfies the condition:

(PN-1) $f_x(t) = H(t) \quad \forall t \in R$ if and only if $x=\theta$;
(PN-2) $f_x(0) = 0$;
(PN-3) for all $\alpha \in R$, $\alpha \neq 0$, we have

$$f_{\alpha x}(t) = f_x(t/|\alpha|) \qquad (\forall t > 0);$$

(PN-4) $f_{x+y}(t_1+t_2) \geqslant \Delta(f_x(t_1),\ f_y(t_2)) \ (\forall t_1, t_2 > 0,\ x, y \in E)$.

Theorem 2

If $(E,\mathcal{F},\Delta)$ is a Menger probabilistic inner product space, then it is a probabilistic normed space.

Proof

By using the mapping $\mathcal{F}$, we can define the mapping f: $E \to \mathcal{D}$ as follows:

$$f_x(t) = \begin{cases} 0 & (t \leqslant 0) \\ F_{x,x}(t^2) & (t > 0) \end{cases} \tag{5.2}$$

We shall now prove that f as defined by (5.2) satisfies the conditions (PN-1) ~ (PN-4).

In fact, the conditions (PN-1) ~ (PN-3) can be derived from (PI-3), (PI-1), and (PI-4) respectively. For given $x, y \in E$, $t_1 > 0$, $t_2 > 0$, let $a = F_{x,x}(t_1^2)$, $b = F_{x,y}(t_1 t_2)$, $c = F_{y,y}(t_2^2)$. Then from (PI-5) we know:

$$\begin{aligned} f_{x+y}(t_1+t_2) &= F_{x+y,x+y}((t_1+t_2)^2) \\ &\geqslant \Delta(\Delta(a,b),\ \Delta(b,c)) = \Delta(a, \Delta(c, \Delta(b,b))) \\ &\geqslant \Delta(a, \Delta(c,b)) = \Delta(\Delta(a,c), b) \qquad \text{(from 5.1)} \\ &\geqslant \Delta(\Delta(a,c), \Delta(a,c)) \geqslant \Delta(a,c) \\ &= \Delta(f_x(t_1),\ f_y(t_2)) \end{aligned}$$

Q.E.D.

Since a Menger probabilistic inner product space is a probabilistic normed space, it is a Hausdorff topological space[3] with topology $\mathcal{T}$ derived from the neighboring system $\{U_p(\varepsilon,\lambda),\ p \in E,\ \varepsilon > 0,\ \lambda > 0\}$, also,

$$U_p(\varepsilon,\lambda) = \{x \in E:\ f_{x-p}(\varepsilon) > 1 - \lambda\}$$

Therefore, a point sequence $\{x_n\}$ in $(E, \mathscr{F}, \Delta)$ is called $\mathscr{F}$-convergent at x; if for given $\varepsilon>0, \lambda>0$, there exists $N=N(\varepsilon,\lambda)$, then when $n \geqslant N$, we have

$$f_{x_n-x}(\varepsilon)>1-\lambda$$

where f is defined by (5.2)

Theorem 3

If $(E, \mathscr{F}, \Delta)$ is a Menger probabilistic inner product space, then for any sequence $\{u_n\} \subset E$, when $u_n \xrightarrow{\mathscr{F}} \theta$, for any $v \in E$ and given $\varepsilon>0, \lambda>0$, there exists $N=N(\varepsilon,\lambda)$ such that when $n \geqslant N$, we have:

$$F_{u_n,v}(\varepsilon)>1-\lambda$$

Proof

Since $\Delta(a,1)=a$, $a \in [0,1]$ and Δ is continuous, for given $\varepsilon>0, \lambda>0$, there exist $a, b \in [0,1]$ such that

$$\Delta(1-a,\ 1-b)>1-\lambda \tag{5.3}$$

Also, since $f_{v,v}(t^2)$ is a distribution function, there exists $t_0>0$ such that

$$F_{v,v}(t_0^2)>1-b,$$

Furthermore, since $u_n \xrightarrow{\mathscr{F}} \theta$, for a and ε/t_0 which satisfy (5.3), there exists n_0 such that when $n \geqslant n_0$, we have:

$$F_{u_n,u_n}((\varepsilon/t_0)^2)>1-a$$

Therefore, from (5.1) we obtain

$$\begin{aligned} F_{u_n,v}(\varepsilon)=F_{u_n,v}(\varepsilon/t_0 \cdot t_0) &\geqslant \Delta(F_{u_n,u_n}(\varepsilon/t_0)^2,\ F_{v,v}(t_0^2)) \\ &\geqslant \Delta(1-a,\ 1-b)>1-\lambda \qquad (v \in E) \end{aligned}$$

Theorem 4

Let $(E, \mathscr{F}, \Delta)$ be a Menger probabilistic inner product space which satisfies the condition:

$$F_{x+y,z}(t) \leqslant \Delta^*(F_{x,z}(r),\ F_{y,z}(s)) \qquad (\forall t \in R;\ x,y,z \in E) \tag{5.4}$$

where $t=r+s$, Δ^* is the conjugate norm of Δ, i.e.,

$$\Delta^*(a,b)=1-\Delta(1-a,\ 1-b) \qquad (\forall a,b\in[0,1])$$

also, assume that $u_n \xrightarrow{\mathscr{F}} u_0 \varepsilon E$, then for any $v \varepsilon E$, we have:

(i) $\lim_{n\to\infty}\inf F_{u_n,v}(t)\geqslant F_{u_0,v}(t) \quad (t\in R)$

(ii) if t is a continuous point of $F_{uo,v}$, then

$$\lim_{n\to\infty} F_{u_n,v}(t)=F_{u_0,v}(t)$$

Proof

Since Δ is continuous, and $\Delta(a,1)=a$ ($a\varepsilon[0,1]$), for an arbitrary $\varepsilon>0$, there exists $\lambda>0$ such that

$$\Delta(1-\lambda,\ F_{u_0,v}(t-\varepsilon))>F_{u_0,v}(t-\varepsilon)-\varepsilon$$

also, when $\varepsilon\downarrow 0$, we have $\lambda\downarrow 0$. Furthermore, since $u_n \xrightarrow{\mathscr{F}} u_0$, i.e., $u_n-u_0 \xrightarrow{\mathscr{F}} \theta$, it follows from Theorem 3 that for any $\varepsilon>0$, and an $\lambda>0$ which satisfies the above condition, there exists n_0 such that when $n\geqslant n_0$, we have:

$$F_{u_0-u_n,v}(\varepsilon+)\geqslant F_{u_0-u_n,v}(\varepsilon)>1-\lambda \tag{5.5}$$

Therefore,

$$\begin{aligned} F_{u_n,v}(t)&\geqslant\Delta(F_{u_n-u_0,v}(\varepsilon),\ F_{u_0,v}(t-\varepsilon)) \\ &\geqslant\Delta(1-\lambda,\ F_{u_0,v}(t-\varepsilon))>F_{u_0,v}(t-\varepsilon)-\varepsilon \qquad (\forall n\geqslant n_0) \end{aligned} \tag{5.6}$$

Also, from condition (5.4) we have:

$$\begin{aligned} F_{u_n,v}(t)&=F_{u_n-u_0+u_0,v}(t)\leqslant 1-\Delta(1-F_{u_n-u_0,v}(-\varepsilon),\ 1-F_{u_0,v}(t+\varepsilon)) \\ &=1-\Delta(F_{u_0-u_n,v}(\varepsilon+),\ 1-F_{u_0,v}(t+\varepsilon)) \end{aligned} \tag{5.7}$$

Since $(E,\mathscr{F},\Delta)$ is the Menger probabilistic inner product space, Δ satisfies the condition $\Delta(t,t)\geqslant t$ ($\forall t\varepsilon[0,1]$), hence $\Delta\geqslant\Delta_m$. It follows from (5.7) that

$$\begin{aligned} F_{u_n,v}(t)&\leqslant 1-(F_{u_0-u_n,v}(\varepsilon+)+1-F_{u_0,v}(t+\varepsilon)-1 \\ &=1-(F_{u_0-u_n,v}(\varepsilon+)-F_{u_0,v}(t+\varepsilon)) \end{aligned}$$

With the aid of (5.5) and (5.6), we obtain from the above expression

$$F_{u_0,v}(t-\varepsilon)-\varepsilon<F_{u_n,v}(t)<\lambda+F_{u_0,v}(t+\varepsilon)$$

therefore,

$$\lim_{n\to\infty}\inf F_{u_n,v}(t) \geqslant F_{u_0,v}(t-\varepsilon)-\varepsilon$$

$$\lim_{n\to\infty}\sup F_{u_n,v}(t) \leqslant F_{u_0,v}(t+\varepsilon)+\lambda$$

Let $\varepsilon \downarrow 0$ and hence $\lambda \downarrow 0$ in the above expressions, we obtain

$$\lim_{n\to\infty}\inf F_{u_n,v}(t) \geqslant F_{u_0,v}(t) \qquad (t \in R)$$

$$\lim_{n\to\infty}\sup F_{u_n,v}(t) \leqslant F_{u_0,v}(t+) \qquad (t \in R)$$

If t is a continuous point of $F_{uo,v}$, one can readily obtain (ii) from the above expressions.

Q.E.D.

VI. Orthogonality

Definition 4.

Let $(E,\mathcal{F},\Delta)$ be a probabilistic inner product space, and $u,v \in (E,\mathcal{F},\Delta)$. u, v are said to be orthogonal if $F_{u,v}(t)=H(t)$ $(\forall t \in R)$. It is denoted by $u \perp v$.

Theorem 5.

The orthogonality of the probabilistic inner product space has the following properties:

(i) $\theta \perp u, \ \forall u \in E$;

(ii) $u \perp v$, then $v \perp u$;

(iii) $u \perp u$, then $u=\theta$;

(iv) $u \perp u_i \ (i=1,2,\cdots,n)$, then $u \perp \sum_{i=1}^{n} u_i$;

(v) If $u \perp v$, then for any $\alpha \in R$, $u \perp \alpha v$;

(vi) Let $(E,\mathcal{F},\Delta)$ be a Menger probabilistic inner product space which satisfies the condition (5.4). Also, assume that $u_n \xrightarrow{\mathcal{F}} u$, $v \perp u_n$ $(n=1,2,...)$ and $F_{u,v}$ is a continuous distribution function, then $u \perp v$.

Proof

The properties (i) ~ (iii) follow directly from conditions (PI-4), (PI-2) and (PI-3). Also, since

$$F_{u,\sum_{i=1}^{n} u_i}(t)=(F_{u,u_1}\oplus F_{u,u_2}\oplus\cdots\oplus F_{u,u_n})(t)$$

$$=(H\oplus H\oplus\cdots\oplus H)(t)=H(t)$$

proof of property (iv) follows.

If $u\perp v$, then for all $\alpha\in R, \alpha>0$, we have:

$$F_{u,\alpha v}(t)=F_{u,v}(t/\alpha)=H(t/\alpha)=H(t) \quad (\forall t\in R)$$

when $\alpha=0$, we obviously have:

$$F_{u,\alpha v}(t)=H(t) \quad (\forall t\in R)$$

when $\alpha<0$, we have:

$$F_{u,\alpha v}(t)=1-F_{u,v}\left(\frac{t}{\alpha}+\right)=1-H\left(\frac{t}{\alpha}+\right)$$

$$=\begin{cases}0 & (\text{when } t\leqslant 0)\\ 1 & (\text{when } t>0)\end{cases}=H(t) \quad (\forall t\in R)$$

hence proof of property (v) follows.

Now we shall prove property(vi). In fact, since $v\perp u_n$ $(n=1,2,\cdots)$, and $F_{u,v}$ is a continuous distribution function, it follows from theorem 4(ii) that

$$H(t)=\lim_{n\to\infty} F_{u_n,v}(t)=F_{u,v}(t) \quad (\forall t\in R)$$

hence $u\perp v$. Q.E.D.

REFERENCES

[1] Zhang Shisheng, "A Theorem on the Stationary Point of Mapping in Probabilistic Inner Product Space", Applied Mathematics and Mechanics, 6, 1 (1985), pp 67-74.

[2] Dumitrescu, C., Un produit scalaire probabiliste, Rev. Roumania Math. Pure et Appl., 26, 3 (1981), 399-404.

[3] Schweizer, B. and A. Sklar, Probabilistic Metric Spaces, North-Holland, New York, Amsterdam, Oxford (1983).

[4] Yu Zhaoyung, Zhu Linhu, "Probabilistic Inner Product Spaces", Science Bulletin, 8(1983), pp 456-459.

3012/7358
CSO: 4008/1027

DISTRIBUTION OF TIME STATISTICS ON PERT

Shanghai ZIRAN ZAZHI [NATURE JOURNAL] in Chinese Vol 9, No 9, Sep 86 pp 713-714

[Article by Wang Xinghua [3769 5281 5478], Xie Tingfan [6200 2656 5672]; paper received 8 Jul 85]

[Text] Let a, b, c be the most optimistic, most conservative and most probable estimates of the time t for completing a task respectively. According to U.S. PERT literature, the random variable t obeys the β distribution on the interval [a,b], i.e., its probability density is of the form: $\beta(x)=$

$$(b-a)^{-p-q-1}B(p+1,\ q+1)^{-1}(x-a)^{p}(b-x)^{q},$$

where

$$B(m,\ n)=\Gamma(m)\Gamma(n)/\Gamma(m+n),\ p>0,\quad q>0,\ p(b-c)=q(c-a).$$

However, Ref.[1] pointed out that the rationale behind this assertion is unclear; "it is hoped that some theoretical research can be done by mathematicians" to provide an explanation.

Of course, an explanation is not a rigorous proof. Nevertheless, in this article, we shall suggest an explanation for the reader's consideration.

In the family of Pearson distributions, the β distribution and only the β distribution satisfies the following characteristics of the statistic t:

i) the compact subset of the probability density f(x) is a finite interval (a,b), and f(a+)=f(b-)=0.

ii) it has a single mode c, $a < c < b$.

The so-called family of Pearson distributions are distributions for which the probability density y=f(x) satisfies the differential equation y'=r(x)y, where $r \in R_{1,2}$, i.e., r(x) is a rational function with first order numerator and second order denominator. The commonly used continuous distributions such as the normal distribution, the χ^2 distribution, the Student's t distribution, the Fisher's Z distribution, the Cauchy distribution all belong to the family of Pearson distributions.

We shall now prove the following argument. According to i), r(x) should have extremal points a and b; according to ii), r(x) should have a zero at c; furthermore, when $x < c$, $r(x) < 0$, when $x > c$, $r(x) > 0$. Therefore,

$$r(x) = d(c-x)/(x-a)(b-x),\ d>0.$$

By expressing r(x) in the form of irreduceable fractions, one obtains

$$r(x) = \frac{p}{x-a} - \frac{q}{b-x},$$

where

$$p = d(c-a)/(b-a) > 0,$$
$$q = d(b-c)/(b-a) > 0.$$

Thus, integration gives $y=A(x-a)^p(b-x)^q$, where A is an integration constant.

From $\int_{-\infty}^{\infty} y dx=1$, A can be determined to be $A=(b-a)^{-p-q-1} B(p+1,q+1)^{-1}$. Also, from (*) $c=\frac{pb+qa}{p+q}$.

REFERENCE

[1] Hua Luogeng, "Comments on Program Evaluation and Review Technique", China Industrial Publishers (1965)

3012/7358
CSO: 4008/1027

PHYSICAL SCIENCES

INTEGRATED 3-PARAMETER DIAGRAM FOR DETERMINING THERMODYNAMIC PROPERTIES OF FLUIDS

Shanghai ZIRAN ZAZHI [NATURE JOURNAL] in Chinese Vol 9, No 10, Oct 86 pp 796-797

[Article by Zhao Guochang [6392 0948 2490], Deng Xiaoxue [6772 1420 7185], Zhu Mingshan [2612 2494 0810]; paper received 16 Aug 85]

[Text] The importance of thermodynamic properties of fluids has motivated recent studies in developing new methods of calculating thermodynamic properties. Among the various methods, the use of computational diagrams is a commonly used engineering method. However, the conventional diagrams given in the literature (e.g., the deviation function diagram, the fugacity coefficient diagram and the compression factor diagram which use T_r as parameter and p_r as absissa) did not take into consideration the internal relationships among the various thermodynamic properties. As a result, when it is necessary to carry out simultaneous calculations of several thermodynamic properties, one must use a number of related diagrams, which is very cumbersome.

The approach used in this paper considers the internal relationships of various thermodynamic properties. It is found that if we introduce the following definitions

$$\left\{\begin{aligned} & X(p_r,T_r)\equiv \int_{0,T_r}^{p_r,T_r}(1-Z)d\ln p_r-\ln p_r \\ & \qquad +2.5,^{①} \\ & Y(p_r,T_r)\equiv \int_{0,T_r}^{p_r,T_r} T_r^2\left(\frac{\partial Z}{\partial T_r}\right)_{p_r} d\ln p_r, \\ & Y'(p_r,T_r)\equiv\frac{1}{T_r}Y(p_r,T_r), \\ & Y'_r(p_r,T_r,T_{r0})=\frac{1}{T_{r0}}Y(p_r,T_r), \end{aligned}\right. \tag{1}$$

then the various thermodynamic properties (deviation in enthalpy, deviation in free enthalpy, deviation in entropy, deviation in internal energy, fugacity coefficient, density, enthalpy difference, entropy difference, internal energy difference, enthalpy e, internal energy e and their thermal and mechanical

components) can be expressed as functions of X,Y,Y', p_r, T_r, V_r (2) and the thermodynamic properties of the corresponding ideal gas. To facilitate computation, we further define

$$\begin{cases} W(T_r,\ T_{r0}) \equiv \dfrac{e^*_{th}(T,\ p)③}{RT_0}, \\ W_h(T_r, T_{r0}) \equiv \dfrac{h^*(T)-h^*(T_0)}{RT_0}, \\ W_s(T_r, T_{r0}) \equiv \dfrac{s^*(T,\ p_0)-s^*(T_0,\ p_0)}{R} \\ \qquad = W_h(T_r,\ T_{r0}) - W(T_r,\ T_{r0}). \end{cases} \tag{2}$$

Thus, the thermodynamic properties can be expressed as

$$\begin{cases} \dfrac{g^*(T,\ p_0)-g(T,\ p)}{RT_c} = T_r\{X(p_r,\ T_r) \\ \qquad +mp_{r0}-2.5\}, \\ \dfrac{h^*(T,\ p_0)-h(T,\ p)}{RT_c} = Y(p_r,\ T_r), \\ \dfrac{s^*(T,\ p_0)-s(T,\ p)}{R} = Y'(p_r,\ T_r) \\ \qquad -X(p_r,T_r)-mp_{r0}+2.5, \\ \dfrac{u^*(T,\ p_0)-u(T,\ p)}{RT_c} = Y(p_r,\ T_r) \\ \qquad +\{p_rV_r(p_r,\ T_r)-T_r\}, \\ \dfrac{a^*(T,\ p_0)-a(T,\ p)}{RT_c} = T_r\{X(p_r,\ T_r) \\ \qquad +mp_{r0}-2.5\}+\{p_r\ V_r\ (p_r,\ T_r) \\ \qquad -T_r\}, \\ m\phi(p_r,T_r) = -\{X(p_r,T_r)+mp_r-2.5\}, \\ \rho(p_r,\ T_r) = \dfrac{p_c}{RT_c}\cdot\dfrac{1}{V_r(p_r,\ T_r)}, \\ \dfrac{h(T,\ p)-h(T_0,\ p_0)}{RT_0} = W_h(T_r,\ T_{r0}) \\ \qquad -\{Y'(p_r,\ T_r,\ T_{r0})-Y'(p_{r0},\ T_{r0})\}, \\ \dfrac{s(T,\ p)-s(T_0,\ p_0)}{R} = W_s(T_r,\ T_{r0}) \\ \qquad -\{Y'(p_r,\ T_r)-Y'(p_{r0},\ T_{r0})\}\ (3) \\ \qquad -\{X(p_{r0},\ T_{r0})-X(p_r,\ T_r)\}, \\ \dfrac{u(T,\ p)-u(T_0,\ p_0)}{RT_0} = W_h(T_r,\ T_{r0}) \\ \qquad -\{Y'(p_r,\ T_r,\ T_{r0})-Y'(p_{r0},\ T_{r0})\} \end{cases} \tag{3}$$

$$
\left\{
\begin{aligned}
&-\frac{1}{T_{r0}}(p_r V_r(p_r, T_r) \\
&\quad - p_{r0} V_r(p_{r0}, T_{r0})\}, \\
&\frac{e_{mech}(T_0, p)}{RT_0} = X(p_{r0}, T_{r0}) \\
&\quad - X(p_r, T_{r0}), \\
&\frac{e_{th}(T, p)}{RT_0} = W(T_r, T_{r0}) \\
&\quad - \{Y'(p_r, T_r, T_{r0}) - Y'(p_r, T_r)\} \\
&\quad - \{X(p_r, T_r) - X(p_r, T_{r0})\}, \\
&\frac{e(T, p)}{RT_0} = W(T_r, T_{r0}) \\
&\quad - \{Y'(p_r, T_r, T_{r0}) - Y'(p_r, T_r)\} \\
&\quad - \{X(p_r, T_r) - X(p_{r0}, T_{r0}\}, \\
&\frac{e_{umech}(T_0, p)}{RT_0} = X(p_{r0}, T_{r0}) - X(p_r, T_r) \\
&\quad + \frac{V_r(p_r, T_{r0})}{T_{r0}}(p_{r0} - p_r), \\
&\frac{e_{uth}(r, p)}{RT_0} = W(T_r, T_{r0}) \\
&\quad - \{Y'(p_r, T_r, T_{r0}) - Y'(p_r, T_r)\} \\
&\quad - \{X(p_r, T_r) - X(p_r, T_{r0})\} \\
&\quad + \frac{1}{T_{r0}}(p_{r0} - p_r)\{V_r(p_r, T_r) \\
&\quad - V_r(p_r, T_{r0})\}, \\
&\frac{e_u(T, p)}{ET_0} = W(T_r, T_{r0}) \\
&\quad - \{Y'(p_r, T_r, T_{r0}) - Y'(p_r, T_r)\} \\
&\quad - \{X(p_r, T_r) - X(p_{r0}, T_{r0})\} \\
&\quad + \frac{V_r(p_r, T_r)}{T_{r0}}(p_{r0} - p_r).
\end{aligned}
\right.
$$

where W, W_k can be selected from any one of the following 3 forms:

If C_p^* is based on the average specific heat:

$$
\left\{
\begin{aligned}
&W(T_r, T_{r0}) = \frac{C_p^*}{R}(T_r/T_{r0} - 1.0 \\
&\qquad - \ln T_r/T_{r0}), \\
&W_h(T_r, T_{r0}) = \frac{C_p^*}{R}(T_r/T_{r0} - 1.0),
\end{aligned}
\right.
\tag{4}
$$

If C_p^* is based on a given specific heat:

$$\begin{cases} W(T_r, T_{r0}) \\ \quad =\dfrac{K}{K-1}(T_r/T_{r0}-1.0-\ln T_r/T_{r0}), \\ W_h(T_r, T_{r0})=\dfrac{K}{K-1}(T_r/T_{r0}-1), \end{cases} \tag{5}$$

If C_p^* is computed from the formula $C_p^*=A+BT+CT^2+DT^3$, then

$$\begin{cases} W(T_r, T_{r0})=\dfrac{1}{RT_0}\Big\{(A-T_0B)(T-T_0) \\ \quad +\dfrac{B-T_0C}{2}(T^2-T_0^2)+\dfrac{C-T_0D}{3} \\ \quad \cdot(T^3-T_0^3)+\dfrac{D}{4}(T^4-T_0^4) \\ \quad -T_0A\ln T/T_0\Big\}, \\ W_h(T_r, T_{r0})=\dfrac{1}{RT_0}\Big\{A(T-T_0) \\ \quad +\dfrac{1}{2}B(T^2-T_0^2)+\dfrac{1}{3}C(T^3-T_0^3) \\ \quad +\dfrac{1}{4}D(T^4-T_0^4)\Big\}. \end{cases} \tag{6}$$

Therefore, by choosing $X(p_r, T_r)$ respectively as the absissa and the ordinate, with p_r, T_r, V_r as parameters, one can use conventional equations to plot the iso-T_r, iso-p_r and iso-V_r curves. Also, by using equations (5) and (6) to generate curves of W and W_k as functions of T_r, T_{ro}, and by generating auxiliary curves for determining $Y'(p_r,T_r)$ (or $Y'(p_r,T_r, T_{ro})$) based on $Y(p_r, T_r)$ and T_r(or T_{ro}), one can construct an integrated diagram for determining the thermodynamic properties.

In this paper, we have used the Lee-Kessler three-parameter equations to construct "an integrated three-parameter diagram for determining the thermodynamic properties of fluids"; the curves are generated using an ai-M/6 microcomputer with an attached Sr 6602 plotter. In this diagram, the range of p_r varies from 0.002 to 15.0, the range of T_r is from 0.55 to 4.5, and the range of V_r is from 0.14 to 200.0; the diagram is clear and easy to read. Also, by using nitrogen, n-butane and isobutane to test the accuracy of the diagram, it is found that the error is less than 1.0 percent over a wide range of temperatures and pressures. Hence the diagram is sufficiently accurate for engineering calculations.

FOOTNOTES

1 The specific parameters in this paper are measured in mols; the constant 2.5 is introduced to avoid negative values of x in the diagram.

2 V_r denotes the ideal specific volume

$$V_r(P_r, T_r) = \frac{P_c V(p, T)}{RT_c}.$$

3 Parameters with "*" refer to ideal gas conditions.

3012/7358
CSO: 4008/1027

PHYSICAL SCIENCES

GENERALIZED COUPLED-MODE EQUATIONS, APPLICATIONS TO FIBER COUPLERS

Hefei ZHONGGUO KEXUE JISHU DAXUE XUEBAO [JOURNAL OF CHINA UNIVERSITY OF SCIENCE AND TECHNOLOGY] in English Vol 16, No 4, Dec 86 pp 427-431

[Article by Qian Jingren [6929 2529 0088], Department of Radio and Electronics; received 1 February 1986]

[Text] Abstract: Generalized coupled-mode equations for two or more coupled weakly-guiding fibres when not well separated, are presented. These equations have been used to study fibre couplers. Compared with the results derived from previous coupled-mode equations, our results are in better agreement with those calculated rigorously by a numerical method.

Coupled-mode equations describing the power transfer between two or more parallel fibres have been derived by Snyder et al[1-3]. In deriving these equations, they considered that fibres are weakly guiding and optically well separated, so the total transverse fields of the composite waveguide can be approximated by a superposition of the fields of each fibre in isolation from the others, namely

$$E(x,y,z) = \sum_k A_k(z) e_k(x,y),$$
$$H(x,y,z) = \sum_k A_k(z) h_k(x,y), \qquad (1)$$

where e_k and h_k are the transverse parts of the modal fields for the k^{th} guided mode. There may be several modes guided on each fibre in isolation, the summations in eqn. (1) are over all the guided modes on all coupled fibres.

In practice, for example, in polished and fused single mode couplers[4,5], to obtain strong coupling, the coupling fibres are touched or nearly touched. Therefore, the validity of eqn. (1) should be checked. Fortunately, the assumption eqn. (1) has already been justified by Wijngaard[6], when he studied two coupled weakly-guiding optical fibres. He has found that eqn. (1) is a remarkably good

approximation even when the cores are touching. Our letter will be based on this point.

First of all, it is necessary to check the orthogonality relation

$$Re\left[\iint_{A_\infty} e_k \times h_i^* \cdot i_z d\Omega\right] = \delta_{ki}, \tag{2}$$

Where A_∞ is the infinite cross-sectional area, δ_{ki} is the Kronecker delta, i_z is the unit vector in the z-direction. Based on this relation, a set of coupled-mode equations were previously derived from Maxwell's equations. However, eqn.(2) is true only for the modes on the same fibre; the modes on different fibres are not orthogonal. Eqn. (2) is a reasonable approximation only when the coupled fibres are well separated.

Based on eqn. (1), we can now proceed to formulate the generalised equations. Using eqn.(2) for modes on the same fibre and

$$g_{Ki} = Re\left[\iint_{A_\infty} e_K \times h_i^* i_z d\Omega\right], \tag{3}$$

for modes on different fibres. according to the procedure mentioned in ref. 1, we have the matrix form of the coupled-mode equations for the coupled fibres:

$$\frac{d}{dz}(GA) + jBGA = -jKA, \tag{4}$$

where matrix G has its diagonal elements equal to unity and off-diagonal elements equal to g_{Ki}, which is zero if k and i are modes on the same fibre; A is the amplitude matrix and K is the coupling matrix with its elements

$$K_{Ki} = \frac{\omega\varepsilon_0}{2}\int_{A_\infty}(n_p^2 - n^2)(e_K^* \cdot e_i + \frac{n_2^2}{n_p^2} e_{zK}^* e_{zi}) d\Omega, \tag{5}$$

where n_p denotes the composite profile and n denotes the profile of the individual fibre on which the k^{th} mode propagates, e_{zK} and e_{zi} are the z-directed components of the modal fields, the matrix B is a diagonal matrix whereas its elements β_K are the propagation constants of the guided modes.

If the composite profile n_p for the coupled fibres does not change along z, eqn.(4) becomes

$$\frac{d}{dz}A + jG^{-1}BGA = -jG^{-1}KA. \tag{6}$$

Eqn. (4) or (6) is a generalised coupled-mode matrix equation, and should be more rigorous in describing the mode coupling between coupled fidres. This will be justified by studying double-core fibres.

A double-core fibre may be formed in a coupler, when two fibres are close to each other. If the two cores are circular and identical as shown in the inset of Figure 1, and if each individual one-core fibre is single moded, then eqn. (6)is reduced to

$$\frac{d}{dz}A_k = -j(\beta+\triangle\beta)A_K - jCA_i \quad (K, i=1,2, i\neq K) \tag{7}$$

where

$$\triangle\beta = \frac{K_{KK}-gK_{Ki}}{1-g^2}, \tag{8}$$

$$C = \frac{K_{Ki}-gK_{KK}}{1-g^2},$$

where $g=g_{12}=g_{21}$, $\beta=\beta_1=\beta_2$, $K_{12}=K_{21}$, $K_{11}=K_{22}$ due to symmetry.

If the individual one-core fibres have step index profiles and are weakly-guiding, i.e.

$$\triangle = \frac{1}{2}\left(1-\frac{n_{e1}^2}{n_{e0}^2}\right) \ll 1 \tag{9}$$

then K_{11} and K_{12} can be approximated by

$$\frac{\rho K_{11}}{\sqrt{2\triangle}} = \frac{U^2}{2(1+d/\rho)\pi V K_1(W)}\left\{\left[\left(\frac{d}{\rho}+1\right)^2\left[K_0^2\left(W+\frac{d}{\rho}W\right)-K_1^2\left(W+\frac{d}{\rho}W\right)\right]\right.\right.$$
$$\left.\left.-\left(\frac{d}{\rho}-1\right)^2\left[K_0^2\left(\frac{d}{\rho}W-W\right)-K_1^2\left(\frac{d}{\rho}W-W\right)\right]\right]\right\}, \tag{10}$$

$$\frac{\rho K_{12}}{\sqrt{2\triangle}} = \frac{U^2}{V^3}\,\frac{K_0(Wd/\rho)}{K_1^2(W)}, \tag{11}$$

where n_{e0} and n_{e1} are the refractive index for core and cladding respectively, ρ is the core radius, V is the waveguide parameters and U and W are modal parameters for core and cladding, respectively.

If the two cores are touching $(d=2\rho)$, the g can be approximated by

$$g \simeq \frac{4}{V}\frac{\rho}{\sqrt{2\triangle}}(K_{11}+K_{12}), \tag{12}$$

The normalised coupling coefficients $\rho k_{11}/\sqrt{2\triangle}$, $\rho k_{12}/\sqrt{2\triangle}$ and g are plotted against V value in Figure 1 in case $d=2\rho$. All these parameters have their maxima within the range $V=1.3-1.8$, before and after which they drop steadily.

It is well known that the coupled modes can be transformed to the normal modes of the double-core fibre[3]. Since the modified propagation constant of the two coupled modes in eqn. (7) are the same, the transverse spatial dependence of the fundamental mode and the second mode of the composite fibre are just the sum and difference of those of the fundamental modes on individual fibres,

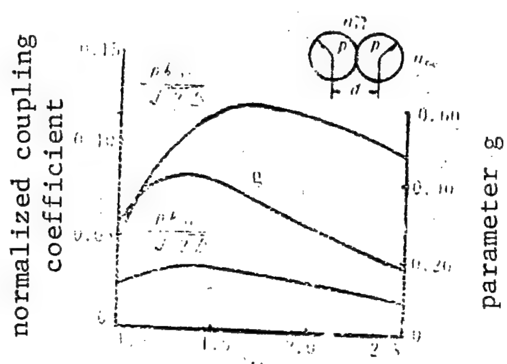

Fig 1 Parameter g and normalised coupling coefficients for $d=2\rho$.

respectively. But the propagation constants for both modes are expressed as follows[1].

$$h_1 = \beta + \frac{k_{12} + k_{11}}{1+g}, \qquad (13)$$
$$h_2 = \beta - \frac{k_{12} - k_{11}}{1-g},$$

The normalised beat-length $(\rho/\sqrt{8\Delta}V)/(h_1 - h_2)$ is evaluated and shown in Figure 2 (unbroken line). The dashed line corresponds to $g=0$ and the dots in the Figure are cited from Wijngaard' s numerical results[6]. It is obvious that our results are found to be in good agreement with his. The discrepancy between both curves is apparent when V is less than 1. 7. It means non-orthogonality between modes should be taken into account at small V-value for touching fibres.

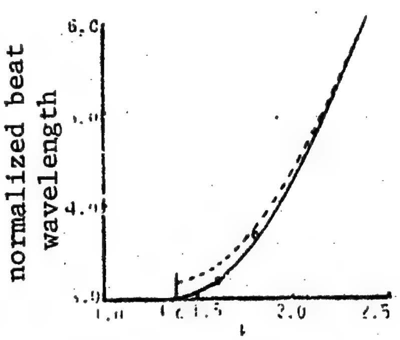

Fig 2 Normalised beat-length calculated by generalised equations (solid—) and by previous equations (dashed---).

The curves in Figure 2 stop at the cut-off V-value for the second mode, which can be easily calculated by solving the following equation:

$$h_2 = \frac{2\pi}{\lambda} n_{e1}, \qquad (14)$$

By using eqns. (9) and (13) in eqn. (14) it is readily shown that

$$\frac{W^2}{2V_e} = \frac{\rho}{\sqrt{2\Delta}}\left(\frac{k_{12} - k_{11}}{1-g}\right), \qquad (15)$$

Using eqns. (10), (11) and approximate expression of W in eqn. (15), its solution V_e is 1.38. This is exactly the same as the recent result given by Love et al[7].

In conclusion, the coupled-mode equations for coupled fibres are generalised for any separation between fibres. Using them, we can obtain satisfactory results for double-core fibre. Compared with the results derived from the previous coupled-mode equations, it seems that the previous equations are valid in describing power transfer even in touching fibre provided $V > 1.7$.

The author wishes to express thanks to professor W. A. Gambling and Dr.D.N. Payne for providing a stimulating research atmosphere, and would like to acknowledge Dr. C. D. Hussey for useful discussions. Financial support from the British Council is also gratefully acknowledged.

References

[1] Snyder, A. W., *J. Opt. Soc. Amer.*, **62** (1972), 1267—1277.

[2] McIntyre, P., Snyder, A. W., *J. Opt. Soc. Amer.*, **63** (1973), 1518—1527.

[3] Snyder, A. W., Love, J. D., Optical waveguide theory, Chapman and Hall, London, 1983

[4] Payne, F. P., Hussey, C. D. Yataki, M. S., *Electron. Lett.*, **21** (1985), 561—563.

[5] Digonnet, M. J. F., Shaw, H. J., *IEEE J. Quant. Electron.*, **QE—18** (1982) , 748—754.

[6] Wijngaard, W., *J. Opt. Soc. Amer.*, **63** (1973), 944—954.

[7] Love, J. D., Ankiewicz, A., *J. Lightwave Technol.*, **LT—3** (1985) , 100—110.

/6091
CSO: 4010/1018

STATUS OF TITANIUM ALLOYS R&D DESCRIBED

Beijing GUOJI HANGKONG [INTERNATIONAL AVIATION] in Chinese No 10, 5 Oct 86 pp 8-11

[Article by Ceng Fanchang [2582 0416 2490]: "Titanium Alloy R&D in China"; first paragraph is source-supplied English abstract]

[Text] Abstract: After a brief chronological description of titanium alloys in aviation industry, the article gives highlights on the achievements in manufacturing of large forgings, in particular, high speed hammer forging, high temperature forging and isothermal die forging. A prospect of titanium alloy development is outlined.

The research and development of titanium alloys for the aviation industry in China began in the 1950's and the effort was centered on the development and application of TC4 (equivalent to Ti-6Al-4V). Systematic studies were made on the melting, casting, forging, heat treatment and machining of the alloy and the relationship between the composition and the performance. Problems in controlling the composition, hydrogen content and the homogeneity of the cast parts have basically been solved. In the early 1960's, compressor disks and blades made of Ti-6Al-4V were applied on the WP6 engine to replace steel at a weight saving of 32 kg. This development marked an important step in the application of titanium alloys to critical aviational components in China.

In the 1970's the research and development of titanium alloys in China entered a new era. Based on the experience of titanium usage in foreign aviation and space industries and the needs of engine development, China developed its own deformable titanium alloys and cast titanium alloys and established a series of titanium alloys of different strength and service temperatures. In the meantime China has engaged in extensive applied research in the metallurgical and mechanical properties of titanium, its failure mechanisms and new manufacture technologies and facilities for titanium alloys. The emphases were placed on casting and forging techniques and the structural and performance changes under different deformation conditions. A number of new forge pressing techniques were developed for the Chinese aviation industry.

I. Hot Die Forging of Titanium Alloy Disks

Experience shows that the rate of deformation during forging plays a role in the thermoplastic and fracture properties of titanium alloys. By properly controlling the parameters, such effects may be reduced to a minimum. The α-β titanium alloys may be formed in a die or formed by hammer forging. In the past it was believed that titanium alloy disks formed by hot die forging had a more homogeneous structure and better mechanical properties. Research results showed that the structure and performance of TC4 and TC11 compressor disks met the engine requirements whether they were formed in a die or stamped, as long as the processes were properly controlled. In hammer forging the temperature can be accurately controlled. By appropriately raising the dye temperature and applying protective lubrication, the deformation may be properly distributed. The hammer forging technique can therefore ensure the homogeneity of the forged parts and give the recrystallization the appearance of a ground glass. The mechanical properties of such forged parts are quite good.

The head velocity of the high energy hammer used in the forging of titanium alloys is 15 m/s, about twice the velocity of ordinary hammer forging. As the hammer velocity increases, the strain rate and the tensile deformation of the alloy also increase. The thermal conductivity of titanium alloy is only about one-fourth to one-third of that of steel. The temperature rise due to local deformation may cause excessive heating and the nonuniform deformation causes pronounced nonhomogeneous strain bands. Such overheating and strain bands are even more serious under higher rates of deformation. For these reasons, hammer forging was for a long time regarded as an inappropriate technique for titanium disks. After extensive tests and research, we have found a method for die forging titanium disks using the high-speed high-energy hammer. Experience showed that TC11 disks meeting the engine requirements can be produced with a high-speed high-energy hammer as long as the die forging steps, the deformation rate, and the impact forces are carefully controlled and the heating temperature is properly reduced. Figure 1 shows a TC11 titanium alloy disk die forged with a 100 ton-m high velocity hammer. Figures 2 and 3 show respectively the 40 ton-m explosive die forge hammer and the TC11 disk produced by the hammer.

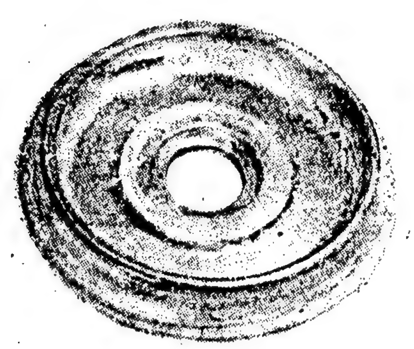

Figure 1. A TC11 titanium disk (505 x 94 mm) forged by a 100 ton-m high velocity hammer

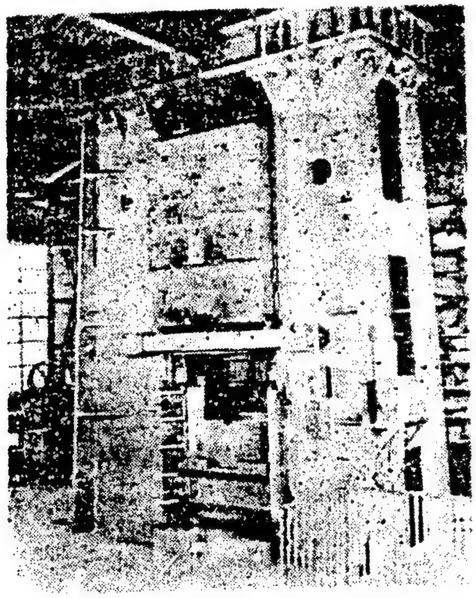

Figure 2. A 40 ton-m explosive die forging hammer

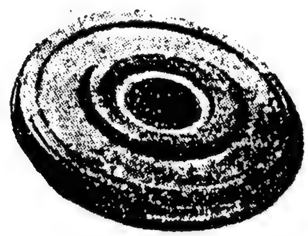

Figure 3. A TC11 titanium disk (510 x 43 mm) forged by the 40 ton-m die forging hammer

II. High Temperature Forging of Titanium Alloys

For α-β titanium alloys, techniques for producing the ingots and blanks, shaping of the blanks and β-forging are widely known. Heating to the temperature of the α-β/β transformation or raising the transformation temperature can substantially increase the plasticity of the alloy and reduce the resistance to deformation; and thereby breaking up the cast structure and reducing the number of forgings required. In the final production process of titanium disk, the β forging technique has not received the proper attention and emphasis. Even in industrially developed nations the users are not confident about the β forging technique. Since this technique is rather complex, processes to ensure the accuracy are not yet complete. Under these conditions it is difficult to achieve processing consistency and product quality. The economic benefits of β forging has not yet been realized. These factors contributed to the sparse attention and application of the β forging technique.

In the last few years China has made considerable progress in the applied research of titanium alloys. The widely accepted and extensively studied

α-β two phase forging is being challenged by the high temperature forging. Research results on sub-β forging, near-β forging and superhigh temperature forging have shown the potential of these new techniques over the conventional forging in the two phase region.

In the high temperature forging of the titanium alloys, the blanks are heated to above the α-β/β temperature and the forging is initiated at high temperature. The forging process may be completed above, at, or below the phase transition temperature. As compared to the two-phase forging, the high temperature forging is done at a higher temperature and completed at a higher temperature. The finishing temperature plays a determining role in the microstructure. Examination of the four types of microstructures (plate-like, network, dual states and equiaxial) shows that the microstructures of the alloys are affected by the deformation temperature and the extent of the deformation. Different desirable mechanical properties may be obtained by controlling the microstructures.

Recent research results here and abroad show that, compared to equiaxial and dual state structures in titanium alloy disks, the network structure has a higher fracture toughness and creep strength, a moderate fatigue strength, and the decreases in the cross-sectional shrinkage and the coefficient of elongation are not significant. The network structure is therefore a desirable structure in terms of the service conditions of the compressor disk and the metallurgical and mechanical behavior under the service conditions. Curved or straight network structures may be obtained by applying superhigh temperature forging, sub-β forging, near-β forging or β-phase forging. The TC6 and TC11 disks manufactured using the above techniques outperform the disks forged in the two phase region in terms of the major performance parameters. Pronounced improvements are achieved in fracture toughness, creep strength, low cycle fatigue, and crack propagation, implying an improved service life and reliability. Studies also show that TC11 compressor disks toughened by near-β deformation not only have the optimum strength-plasticity-toughness combination, but also have much better fracture toughness and fatigue properties, especially at high temperatures. For example, the performance data collected at 520°C-530°C on such disks are equivalent to those of a conventional two-phase forged disk at 500°C. This shows that improved processing can improve the material performance without changing the alloy composition and such improvements can lead to substantial economic benefits.

Tables 1 and 2 show the test results of high temperature forged TC6 and TC11 disks. Compressor disks produced by this new technique have passed quality evaluation and will soon be put on the new engine for long-term testing.

Another feature about high temperature forging is that the deformation resistance of the alloy decreases considerably. Compared to the two-phase forging, the deformation resistance at high temperature is 1.3-2.2 times lower. This helps to improve the part tolerance and reduce the cost. The Chinese aviation industry is very active in the research of high temperature forging of titanium alloys. In addition to theoretical and applied research on the heat treatment, microstructure, and mechanical properties, emphasis is

also placed on the precise control of heating temperature and deformation. The goal is to control the quality under a production environment to ensure reliability and repeatability.

Table 1. Mechanical Properties of TC6 Ti Alloy Disk Under Different Heat Treatments

Forging technique	Heat treatment	Room temp tensile σ_b MPa	Room temp tensile δ %	Room temp tensile ψ %	400°C tensile σ_b MPa	400°C tensile δ %	400°C tensile ψ %	Fracture toughness K_{IC} MPa-mm$^{\frac{1}{2}}$	Impact toughness a_k J/cm^2
Sub-β forging	Isothermal annealing	1079	14	24	824	16	57	2550	49
	Double annealing	1196	13	22	883	16	53	2187	53
Conventional two-phase forging	Isothermal annealing	1040	20	52	775	19	59	1765	57
	Double annealing	1157	16	50	834	18	66	1275	64

Table 2. Mechanical Properties of TC11 Ti Alloy Disk Under Different Heat Treatments

Forging technique	Room temp tensile				Thermal stability: 500°C, 100 hrs				Thermal stability: 500°C, 100 hrs, 343 MPa			
	σ_b MPa	$\sigma_{0.2}$ MPa	δ %	ψ %	σ_b MPa	$\sigma_{0.2}$ MPa	δ %	ψ %	σ_b MPa	$\sigma_{0.2}$ MPa	δ %	ψ %
Conventional	1062	990	14.3	43.2	1088	/	14.0	37.7	1066	/	12.5	38.5
Near-β	1098	1053	16.8	44.2	1120	1054	15.0	37.7	1111	1032	14.8	37.6

Forging technique	Sustained σ_{100} (MPa) 500°C	Sustained σ_{100} (MPa) 520°C	500°C creep σ(MPa)	500°C creep t(hr)	500°C creep δ_r(%)
Conventional	598	/	343	100	0.133
Near-β	706	608	343	100	0.104

Forging technique	Low cycle fatigue: Temp, °C	R	K_t	Freq, min^{-1}	σ_{max}(MPa)	Nf
Conventional	Room temp	0.1	2.4	10	716	6,658
	500°C	0.1	2.4	10	490	6,069
Near-β	Room temp	0.1	2.4	10	716	11,240
	500°C	0.1	2.4	10	490	9,102
	520°C	0.1	2.4	10	490	16,036

III. Isothermal Die Forging of Titanium Alloys

The high cost of titanium alloys was once a limiting factor for their broad usage. With improved technology, problems in high temperature die material, lubricant, and the control of superplasticity have been solved. A high efficiency isothermal die forging technique has now reached the industrial application stage. This technique provides considerable economic benefits and makes increased usage of titanium alloys possible.

In the hot work of titanium alloys it is important to keep the blank hot. This can be done by preheating the die, applying protective lubricant on the blank, or making use of the heating effect during high speed deformation. However, the best method is to heat the die to the same temperature as the deforming metal so that the blank temperature will not drop during the process. This is the isothermal die forging technique developed over the last 20 years.

It has been shown that isothermal forging can greatly reduce the deformation resistance. Since the alloy is maintained in its optimum plastic state during the entire process, the deformation mechanisms are grain boundary glide and rotation. Near the end of isothermal forging the flow of metal takes place by creeping under the superplastic condition. In the isothermal die forging of the integral TC4 turbine (it has 39 blades, a disk diameter of 93 mm and an outer diameter of 120 mm with the blades), the pressure is only 10-13 kg/mm^2, and the load of the hydraulic press is 150 tons.

Glass lubricant can greatly improve the friction between the metal and the die so that the deformation is uniform and the surface oxidation is prevented. These are the necessary conditions in the isothermal die forging of titanium alloys. The Chinese aviation industry has produced a series of products using the protective lubricant. The "FR" series glass lubricants allow the precision forging of titanium blades, disks and other parts.

Another important condition is to heat the die to 900-1100°C and maintain this temperature. Commonly used methods are heating in a resistance furnace and inductive heating. A resistance furnace can only heat small or medium-sized dies and is not economical for larger dies. For larger dies inductive heating is more economical. The successful development of the high temperature die material solved a key problem for the isothermal die forging of titanium. The material must have a higher strength than titanium at the forging temperature and must not oxidize over a long service period. From an economic viewpoint, cast nickel based alloy used for making turbine guide blades for the hot section of the engine is a good die material. Such material may be obtained from aircraft engine plates and the dies of various shapes may be cast from vacuum-remelted turbine guide blades. Most of the dies used in China are made this way. In certain cases where the part shape is complex, ceramic dies may be used.

Figure 4 shows the TC4 blade and TC4 disk made by isothermal die forging. Other parts made this way are the TC11 compressor disk (415 x 50 mm) and the TC4 adoptor seat (150 mm diameter by 5-7 mm).

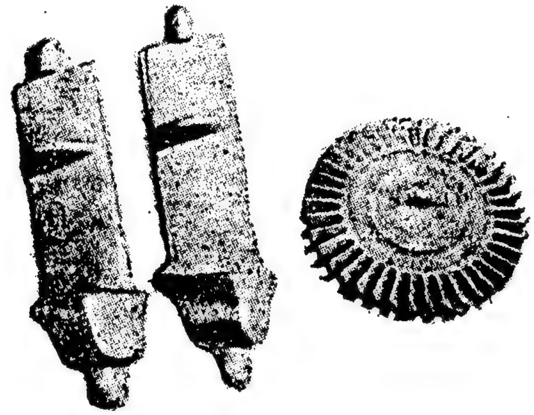

Figure 4. TC4 blades and disk made by isothermal die forging

After 20 years of effort, the Chinese aircraft and engine industry has achieved breakthroughs in titanium alloy technology and application. Titanium alloys in jet engines and aircraft have now reached 13 percent and 4 percent by weight respectively. The batch production of titanium forged parts and their quality control have approached or achieved advanced world standards. For example the state-operated Hongyuan Aviation Forging Plant has become a production supplier of forged titanium parts for Boeing Company and other forging plants are also expanding their sales on the international market. Compared to the advanced world standards, the production and application of titanium alloys in China still have a way to go. The author believes that China should work on the following areas:

1. Improve the material structure and the overall performance of titanium alloys by using new techniques;

2. Systematic and complete application and production methods should be developed for titanium alloys;

3. Adopt internationally accepted material standards and quality control methods;

4. Work closely with the material industry departments in developing new titanium alloys of greater toughness and temperature resistance and promoting the use of cast titanium alloys;

5. Make an effort to broaden the application of titanium alloys in aircraft and engines.

With these efforts, the Chinese titanium industry and aviation industry will enjoy greater developments.

The author acknowledges the assistance provided by Zhang Zhifang [1728 1807 2455], Cao Chunxiao [2580 2504 2556], Liu Jianyu [0491 1696 1342], Yin Weicheng [1438 4850 1004], Li Guangyuan [2621 0342 6678], and Zhou Yigang [0719 5030 0474].

9698/6091
CSO: 4008/14

INFLUENCE OF BORON ON POROSITY IN NICKEL-BASE SUPERALLOY CASTINGS

Beijing JINSHU XUEBAO [ACTA METALLURGICA SINICA] in Chinese Vol 21, No 1, 18 Feb 85 pp A1-A8

[Article by Zhu Yaoxiao [2612 3613 1366], Zhang Shunnan [1728 7311 0589], Xu Leying [1776 2867 5391], Tong Yingjie [0157 2867 2638], Ning Xiuzhen [1337 4423 3791], Liu Zezhou [0491 3419 3166], Hou Cuiping [0186 5050 5493], and Bi Jing [0398 2417] of the Institute of Metal Research, Chinese Academy of Sciences, Shengyang: "The Influence of Boron on the Porosity of Cast Ni-Based Superalloys"; first paragraph is source-supplied English abstract]

[Text] Abstract: The influence of the boron content on the solidification and on the porosity formation of cast Ni-based superalloys has been examined. Because the solubility of boron in the gamma-phase solution is quite limited, boron may be enriched in the melt at the front of the frozen solid during solidification. For superalloys containing more B, say 0.1 percent, the solidified grain may be surrounded by a much lower melting point liquid coating enriched with B to as high as 1 percent. Metallurgical examinations of the microstructures revealed interconnected and continuous "web-like filling channels" that expanded the temperature range of the molten state and reduced the residual amount of liquid unable to fill the pores. As a result, both the performance and the porosity reduction of the cast superalloys were realized. The liquid pools in the alloys were smaller and isolated and microporosities were finely distributed. For superalloys of normal boron content, say about 0.01 percent, the boron was not enriched enough to form the liquid webs. The solidified dendritic grains may be interconnected rather readily along certain fast growing directions, and the residual liquids formed isolated pools. Such unsolidified liquid pools may account for as much as 30 percent of the alloy volume and these inaccessible pools led to serious porosity.

I. Introduction

Nickel-based casting alloys are the principal materials for gas turbine blades in aircrafts and ships. The quality requirements for the service realiability of the blades are very stringent. Highly alloyed Ni-based superalloys generally have poor castibility and tend to have serious porosity problems. In order to reduce porosity, a large temperature gradient is often used at the solidification zone in the production of the blades; but this tend to cause

columnar grains and a large number of blades have been discarded due to porosity or columnar grains. An improved castibility of the Ni-based alloys is therefore essential for better blade performance and yield.

Extensive experimental results and theoretical analysis[1-3] have shown that, by adding small amounts of boron, the solidification temperature zone (the two-phase zone) and the tendency for forming porosity were increased. However, it was discovered recently[4] that, when the boron content was increased to 0.1-0.2 percent, the tendency for porosity was greatly reduced even though the temperature gap became greater. This discovery has generated great interest both in applications and in the theory of porosity formation. As a result, a number of high boron (0.1 wt %) Ni-based superalloys were developed and their interaction mechanisms were investigated[5-7].

Since most high-boron alloys have a low carbon content, some researchers believed that the reduction in porosity was caused mainly by the elimination of the metal carbides that were plugging the filling channels[8]. But the fact is that porosities in low-carbon, low-boron alloys are still very serious[6]. It can therefore be interpreted that the role of boron is to increase the $(\gamma + \gamma')$ eutectic, and thereby reduces porosity. Another viewpoint was that boron modified the final solidification characteristics of the alloys and porosity was reduced as a result. In any case it is not clear why boron reduces the tendency to form porosity. We have made further investigation of the problem by studying the effects of boron on the solidification process.

II. Experimental Method

Compositions of the alloys studied are listed in Table 1. In order to be sure that the base compositions of the alloys are consistent, we prepared the base metals and then added the boron.

Table 1 Chemical composition of superalloys tested, wt-%

Alloy code	C	Cr	Co	W	Mo	Nb	Ta	Al	Ti	B
I	0.022	15.91	8.71	2.54	1.77	0.82	1.62	4.01	3.96	0
II	0.022	15.91	8.71	2.54	1.77	0.82	1.62	4.01	3.96	0.01
III	0.022	15.91	8.71	2.54	1.77	0.82	1.62	4.01	3.96	0.1
IV	0.022	15.91	8.71	2.54	1.77	0.82	1.62	4.01	3.96	0.2
V	0.022	15.91	8.71	2.54	1.77	0.82	1.62	3.0	3.0	0.1
VI	0.022	15.91	8.71	2.54	1.77	0.82	1.62	4.0	4.0	1.0

The samples were cut into 10x15x15mm pieces, placed in a graphite crucible, and then melted and solidified in a silicon carbide tube furnace. The samples were first heated to 1420°C and maintained for 5 minutes. They were then slowly cooled to different temperatures and kept there for 15 minutes. Finally they were rapidly quenched in water.

Samples for porosity and grain size measurements were poured into molds of direction blades of industrial gas turbines in an induction furnace. The

pouring mold consisted of four blades, each blade was about 1.1 kg and the entire pouring system weighed 9 kg. The casted parts were then sectioned and analyzed.

The metallurgical samples were etched in a water solution of H_3PO_3 and H_2SO_4. For macroscopic examination the samples were etched in a 1:1 HCl and H_2O_2 solution. The contents of the phases were determined by metallurgical weighing and the porosity contents were determined by quantitative metallography. The distributions of the elements in the alloys were measured by electron and ion probes.

III. Results and Discussion

Table 2 shows the effects of B, Al, and Ti on the solidification and porosity of the superalloys tested. When the Al and Ti contents and the other compositions were kept the same (Alloys I-IV, VI), boron decreased the crystallization initiation temperature; but the temperature rapidly dropped to 1240°C only when the boron content was increased to 0.1-0.2 wt%. For 0-0.01 wt% boron, the $(\gamma + \gamma')$ eutectic temperature was not reduced but the final solidification temperature was decreased considerably. When the boron content was increased to 0.1-0.2 wt%, these two temperatures remained basically the same. Boron increased the eutectic of $(\gamma + \gamma')$ and $(\gamma + M_3B_2)$ and expanded the two-phase zone; but the zone actually shrinked at higher (1 wt%) boron content.

Table 2 Effect of B, Al or Ti content on solidification and porosity of superalloys tested

Alloy code	Starting solid temp., °C	$\gamma+\gamma'$ Eutectic temp., °C	$\gamma+\gamma'$ wt-%	$\gamma+M_3B_2$ Eutectic temp., °C	$\gamma+M_3B_2$ wt-%	Terminal solid temp., °C	Temp. gap °C	Blade porosity %
I	1315	1220	2	—	—	1210	105	—
II	1310	1220	2	—	—	1180	130	0.38
III	1300	1190	9	1190	2	1150	150	0.1
IV	1300	1190	10	1190	3	1150	150	—
V	1325	1150	4	1150	1	1150	175	0.13
VI	1240	1190	40	1200	25	1120	120	—

Note: Blade casting at temp. 1420°C and shell temp. 900°C.

By comparing the data on alloys V and III in Table 2, one observes that decreasing Al and Ti contents raised the initial crystallization temperature of the alloys and, at the same time, greatly increased the eutectic reaction temperature of $(\gamma + \gamma')$ and $(\gamma + M_3B_2)$, raised the temperature gap to 175°C and decreased the weight percents of the eutectics.

Table 2 also lists the porosity levels of alloys II, III, and V. The low Al and Ti alloy V was low in $(\gamma + \gamma')$ eutectic and had an extremely large two-phase zone. The high Al and Ti alloy III had higher $(\gamma + \gamma')$ eutectic and a large two-phase zone. Both alloys III and V had a low level of porosity. The low boron alloy II had a narrow two-phase zone and serious

porosity. Therefore, at high boron levels, the size of the two-phase zone and the amount of the eutectic are not the major factors affecting the formation of porosity; and it is incorrect to attribute the improvement of porosity to the increased eutectic by the addition of boron.

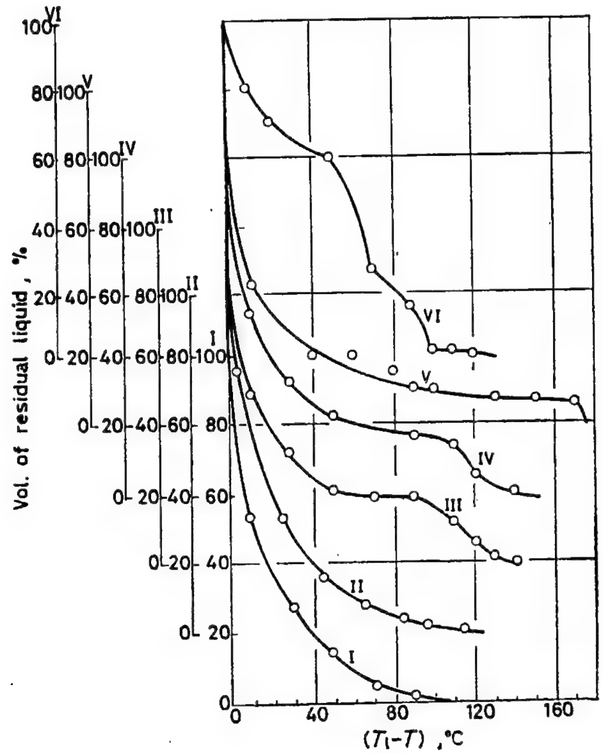

Fig. 1 Volume of residual liquid *vs* slow solidification temperature range
T_l —Liquidus temperature; T—Quenching temperature

Code	I	II	III	IV	VI	V
B, wt-%	0	0.01	0.10	0.20	1.00	0.10
Al	4	4	4	4	4	3
Ti	4	4	4	4	4	3

Figure 1 shows the volume of the residual liquid versus the solidification temperature range (T_l - T). With the exception of the 1 wt% alloy VI, all the alloys shared some common features in the early stage of the solidification. In the first 20-30°C, 60-70 percent of the liquid solidified into the gamma solid solution. The behaviors differed in the late stage of solidification. In boron-free and low boron alloys the solidification gradually continued as the solidification temperature increased until all the liquid had solidified. In high boron alloys the solidification and the temperature range almost halted for a rather long period of time. In alloys III and V with a high level of Al and Ti, a fair amount (about 15 percent) of residual liquid existed during the temporary holding period; whereas in low Al and Ti alloys there were only about 7-10 percent of residual liquid in this

period. When the temperature was decreased to a low level in the high boron alloys for the eutectic reactions to take place, all the residual liquids quickly solidified.

Based on the solidification behaviors of the high boron, high Al and Ti alloys, it was proposed that[7] the higher level of residual liquid in the late stage of the solidification might have improved the filling and there reduced the porosity content. It was also believed that the filling power was directly proportional to (V^3/S^2), where V is the volume of the residual liquid and S is the solid-liquid interface ration. According to the measurement results of Ref. 7, high boron alloys had large V and S, but the low boron alloys had smaller V and S. Because the dependence is to the third power of V and the second power of S, V is the major determining factor and the high boron alloys therefore have a lower level of porosity. However, the high boron alloy with low levels of Al and Ti (alloy V) had a small V and a large S and yet a low level of porosity (see Table 2). The argument of Ref. 7 cannot explain this result. Reference 7 correctly argued that boron modified the solidification behavior of the superalloys and improved the filling ability in the late stage of solidification, but incorrectly stated the criterion for the filling ability. Porosity depends critically on when the channels are blocked and how much residual liquids are left.

The solubility of boron in the gamma solid solution is extremely low. When the alloy solidifies boron is squeezed out of the gamma solid solution into the residual liquid and concentrates in the liquid at the front of the crystallizing solid. This behavior is the same in low boron and high boron alloys but the boron contents in the residual liquids are different. For an enrichment factor of 10, the contents are 0.1 wt% and 1 wt% for the low and high boron alloys respectively. According to Table 2, the drop of the liquidus curve in the 0.1 wt% alloy is only from 1310°C to 1300°C, but the liquidus curve of the 1 wt% alloy has dropped to 1240°C. It is therefore reasonable to assume that, in the solidification of the high boron alloys, the front of the solidifying solid may be surrounded by a layer of high boron, low melting liquid.

In order to verify the existence of the high boron liquid layer, elemental distributions of a solidifying alloy III (0.1 wt% boron) were measured with a microprobe and the results are shown in Fig. 2. The liquid at the front of the solid in alloy III was not only enriched in Nb and Ti, but also in B. All these elements helped to lower the melting point. The enrichment of boron in the liquid in front of the solid was also verified by using an ion probe, as shown in Fig. 3.

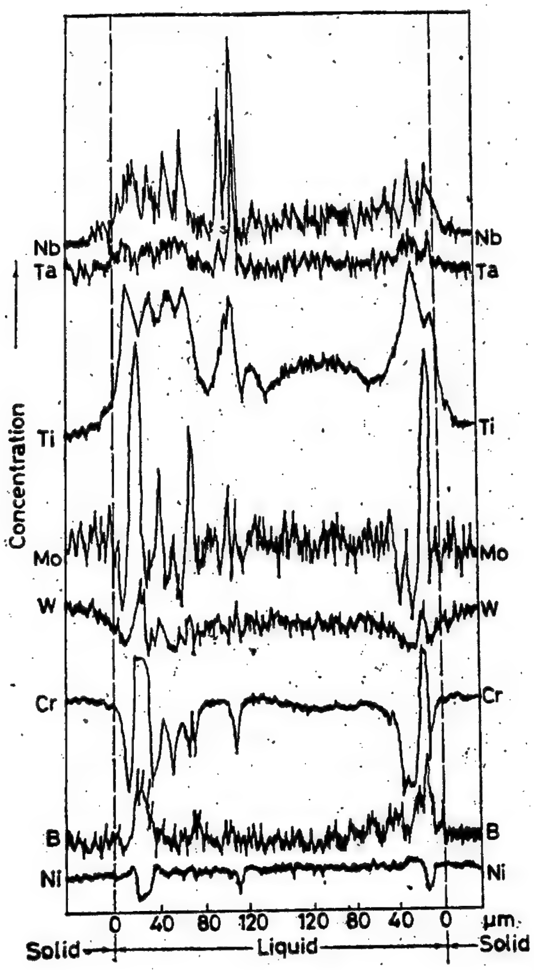

Fig. 2 Distribution of different elements in a partial solodified alloy III EMPA 1420°C 5 min, slowly cooled to 1290°C 15 min, W.Q.

Fig. 3 Distribution of B in a partial solidified alloy III ion probe analysis
Same specimen used as Fig. 2

Alloy III with 0.1 wt% boron has a high-boron-content liquid layer, would this alloy have a low melting point? Figure 4 (see photoplate A1) shows the microstructures of samples with different boron contents slowly cooled from 1420°C/5min to 1290°C/15min and water quenched. All the samples have basically the same structure: solidified gamma phase solid solution formed during the slow cooling and the residual liquid (quench structure), but the quench structures of the boron-free alloy I, the low-boron alloy II and the high-boron alloys III and IV are distinctly different. When the residual liquids in the boron-free and low-boron alloys freeze, the growth is usually a continuation from the gamma solid into the residual liquid. In high-boron alloys the growth usually nucleates from within the residual liquid. This shows that there is indeed a layer of low melting point liquid at the leading edge of the gamma solid solution of high-boron alloys. The quenching process

thwarted the rapid growth of the gamma solid solution into the residual liquid and the higher-melting center of the residual liquid there forms nucleation sites and crystal growth.

Since the freezing solids in 0.1-0.2 wt% alloys are surrounded by a layer of high boron content low melting liquid, the grains and the dendrites are separated by a layer of low melting liquid and cannot join each other. Such low melting point liquids form web-like channels. These channels are connected to the source of liquids and therefore facilitate filling, as shown in Fig. 5 (see photoplate A1). The continuity of the channels only begin to break up when the residual liquid drops to 10-15 percent by weight. In other words, the residual liquid in alloys with 0.1-0.2 wt% boron is about 15 percent.

The behavior in boron-free and 0.01 wt% boron superalloys is different. Because the grains and dendrites are not separated by a low melting point liquid, they quickly join together in the easy growth directions and block the channels, as shown in Fig. 6 (see photoplate A1). The volume of the residual liquid can be as high as 30 percent.

When the uncompensatory residual liquids freeze, porosities are formed. These porosities are formed mostly by the shrinkage upon cooling and solidification. The temperature coefficient of contraction (α) of the liquid is usually small. For steel it is about 1.5×10^{-4}. The contraction coefficient (β) for solidification is much greater; for steel it is about 2×10^{-2}. Therefore, porosities are usually formed by solidification shrinkage. When the residual liquid remains unfrozen over a large range of temperature, the thermal contraction effect of the liquid cannot be ignored either. Porosity can therefore be estimated using the following formulas:

$$\varepsilon_v = \varepsilon_f + \varepsilon_s$$

$$\varepsilon_f = \alpha \int_{T_1}^{T_2} f(T) \mathrm{d}T$$

$$\varepsilon_s = L \times \beta$$

where ε_v is the porosity volume fraction, ε_f is the fractional thermal contraction, ε_s is the fractional solidification contraction, L is the uncompensatory residual liquid volume, is the coefficient of thermal contraction of the liquid (1.5×10^{-4}). β is the coefficient of solidification contraction (2×10^{-2}), f(T) is the temperature distribution function of the residual liquid, T_2 is the starting temperature when the liquid can no longer fill the pores and T_1 is the terminal solid temperature.

Using the formulas above, porosities in alloys with different B, Al, and Ti contents are calculated and the results are listed in Table 3. Alloys with high contents of Al and Ti and 0.1-0.2 wt% boron have a low volume of residual liquid (15 wt%) and small temperature range in which the pores cannot be filled (40°C); as a result, they have the lowest porosity level (0.32

percent). Low Al and Ti alloys with 0.1 wt% boron have a lower residual liquid volume (10 percent) but a large freezing temperature range (100°C), these alloys have a slightly higher level of porosity (0.344 percent). The boron-free alloy (I) and the 0.01 wt% boron alloy (II) have a large volume of residual liquid (30 percent) and also a large range of freezing temperature (75-100°C), they are most susceptible to porosity formation (0.68-0.71 percent). The temperature range of alloy II (100°C) is greater than that of alloy I (75°C), the former therefore has a higher (0.71 percent) than the latter (0.68 percent).

Table 3 Influence of B, Al and Ti contents on solidification parameters and porosity formation tendency

Alloy code	L %	T_f °C	T_2 °C	T_1 °C	$T_f - T_2$ °C	$T_2 - T_1$ °C	$\int_{T_1}^{T_2} f(T)dT$	ε_s %	ε_f %	ε_v %
I	30	1315	1285	1210	30	75	5.5	0.6	0.08	0.68
II	30	1310	1280	1180	30	100	7.5	0.6	0.11	0.71
III	15	1300	1190	1150	110	40	1.5	0.3	0.02	0.32
IV	15	1300	1190	1150	110	40	1.5	0.3	0.02	0.32
V	10	1325	1250	1150	75	100	9.6	0.2	0.144	0.344

Note: L—Residual liquid unable to fill the pores; T_f —Starting solid temperature; T_2—Starting temperature unable to fill the pores; T_1—Terminal solid temperature; ε_f —Liquid shrinkage fraction; ε_v —porosity volume fraction; ε_s —Solidified shrinkage fraction.

In order to assess the effects of B, Al, and Ti on the actual porosity level in the blades, we performed experimental tests. The casting conditions were: pouring temperature was 1420°C, the mold temperature was 900°C, and the results are listed in Table 4. These results show that the calculation method is basically correct. The alloy with 0.1-0.2 wt% B has a low porosity volume fraction and a large number of small pores. The alloy with 0.01 wt% B has a high volume fraction of porosity and a smaller number of larger pores. Alloy V with 0.1 wt% boron and low Al and Ti contents has slightly more porosity than alloy III with 0.1 wt% boron and a higher content of Al and Ti.

Table 4 Influence of B, Al and Ti contents on porosity of precision casting blade

Alloy code	Position	Total no. of pores	Porosity %	250μm² pores no.	250μm² pores Area %	Total area of largest pores μm²
V	Lower	1678	0.13	12	0.02	2474
	Upper	833	0.06	3	0.01	754
III	Lower	1274	0.10	6	0.01	805
	Upper	472	0.06	9	0.02	1053
II	Lower	911	0.38	53	0.31	17739
	Upper	574	0.19	85	0.13	2487

Note: Pouring temperature 1420°C, mold temperature 900°C.

Porosity in actual parts also depends on the part shape, the design and layout of the pouring system, and the casting conditions. A low porosity alloy should not only yield a low level of porosity under specific casting condition but also under adverse casting conditions. As described above, such an alloy should have a low volume of residual liquid, a narrow range of unfillable solidification zone and a large temperature range of $T_{liquid}-T_2$. Table 3 shows that the high Al and Ti alloy III with 0.1 wt% boron has a temperature gap of 110°C and is most adaptable to various casting conditions. The low Al and Ti alloy V with 0.1 wt% boron has a temperature gap of 75°C and a lower adaptability to various casting conditions. The temperature gap in alloys I and II with 0.01 wt% of boron is only 30°C and these alloys are the least adaptable to casting condition variations. The low boron (0.01 wt%) alloys tend to have serious porosity problems and even blow-holes when they are used in casting parts with nonuniform thickness and when the casting conditions fluctuate. High boron (0.1 wt%) alloys do not tend to have these problems.

IV. Conclusions

When Ni-based superalloys with a high boron content (0.1 wt%) solidify, the freezing solid is surrounded by a low melting, boron-enriched liquid layer. This liquid forms web-like filling channels, which increases the pore-filling temperature range and reduces the volume of the residual liquid. As a result, such high boron alloys tend to have low porosity and perform better under different casting conditions. In contrast, the dendrites in boron-free and low boron (0.01 wt%) alloys quickly join together and form relatively large and isolated liquid pools. These inaccessible liquid pools cause serious porosity problems.

REFERENCES

1. R.P. Elliot, "Constitution of Binary Alloys," 1st Suppl., McGraw-Hill, New York, 1965, p 127.

2. C.J. Burton, "Superalloys, Metallurgy and Manufacture," Proc. 3rd Int. Symp., eds. B.H. Kear, et al, Baton Rouge Claitor's Publ. Division, 1976, p 147.

3. K.C. Antony and J.F. Radavich, ibid., p 137.

4. D.H. Maxwell, J.F. Baldwin and J.F. Radavich, "Materials Science Symposium," Cincinnati, 1975. Paper 56, p 322.

5. C.A. Hammersley, METALLUGICA, 45 (1978), No 2, p 105.

6. M.R. Edwards, "Superalloys 1980," Proc. 4th Int. Symp. on Superalloys, edited by J.K. Tien, S.T. Wlodek, et al, ASM p 295.

7. L. Ouichou, F. Lavaud and G. Lesould, ibid, p 235.

8. G. L. R. Durbar, High Temperature Alloys for Gas Turbines, Applied Science Publ., London, 1978, p 459.

9698/7358
CSO: 4008/1026

EFFECTS OF INJECTION OF FREE ELECTRON LASERS ON AXIAL VELOCITY SPREAD OF BEAMS

Shanghai ZHONGGUO JIGUANG [CHINESE JOURNAL OF LASERS] in Chinese Vol. 13, No. 11, 20 Nov 86, pp 671-674, 682

[Article by Wang Yuandian [3769 0337 3013] of the Institute of Space Physics, Chinese Academy of Sciences; manuscript received 19 Aug 85]

[Text] Abstract: An electron beam can be injected into the interaction zone of a free-electron laser adiabatically or non-adiabatically. Non-adiabatic injection is preferred. For free-electron lasers with axial magnetic fields, initial perpendicular velocities can induce axial velocity fluctuations. In order to reduce the fluctuation amplitude, a step-like axial magnetic field can be applied for cooling the perpendicular temperature of the beam, for which proper selection of system parameters is necessary.

I. Introduction

Ensuring the normal operation of free-electron lasers requires a high quality electron beam. Aside from making the energy, intensity, and cross sectional parameters satisfy design requirements, an important index is the degree of longitudinal energy dispersion. If the energy dispersion is great then it can cancel out the coherence of collective effects, lowering gain and efficiency.

The limited emission of the electron beam, the spatial charge effects of high density electron beams, and the presence of a fluctuator magnetic field gradient can effect the size of the degree of longitudinal energy dispersion. When there is an axial magnetic field, there is a strong coupling between the electron's motion in the fluctuating field and the motion around the coiled axial magnetic field. This kind of coupling can cause periodic variations to appear in the longitudinal velocity of the electrons.

This paper studies the effect of electron beam injection methods on the degree of longitudinal velocity dispersion. By solving the motion laws of electron beams passing through a transition zone, the following results can be obtained: non-adiabatic injection leads to longitudinal velocity fluctuations with position or time. Since these are not desired, generally adiabatic injection is preferred.

II. Electron Beam Injection Analysis

In general, electron beam injection methods can be divided into adiabatic injection and non-adiabatic injection. Adiabatic injection means that in the entire process of electrons passing through the transition zone entering the interaction zone they move adiabatically and do not vary is ensured. To realize adiabatic injection, the transition zone must be sufficiently long and the magnetic field variation of the fluctuator guide section must be slow. Non-adiabatic injection is exactly opposite, since the transition zone fluctuation field varies more quickly, adiabatic invariance is not established.

First we discuss the situation of a non-axial magnetic field. Supposing that the wave length of transition zone fluctuation field does not change while the amplitude gradually increases, then the fluctuation field can be written as

$$\boldsymbol{B}_w = B_w(z)\,(\hat{e}_x \cos k_0 z + \hat{e}_y \sin k_0 z) \tag{1}$$

Supposing that $B_w(z)$ is increasing in exponential form, then we can write $B_w(z)=B_{w0}[1-\exp(-z/L_0)]$, L_0 is the length of the transition zone. From the motion equation of electrons

$$\frac{d\boldsymbol{p}}{dt} = -e\frac{\boldsymbol{v}\times\boldsymbol{B}_w}{c} \tag{2}$$

we can derive the momentum p = constant. Substituted in $p^+=p_x iP_y$, making $dz=v_z dt$, from formulae (1) and (2) we can get

$$\frac{dp^+}{dz} = -i\frac{eB_w(z)}{c}e^{ik_0 z} \tag{3}$$

Integrating equation (3) gives

$$p^+ = p_0^+ - i\frac{eB_{w0}}{c\left(\frac{1}{L_0}-ik_0\right)}\left(e^{-\left(\frac{1}{L_0}-ik_0\right)z}-1\right) - \frac{eB_{w0}}{ck_0}\left(e^{ik_0 z}-1\right) \tag{4}$$

in which $p_0^+ = p_{x0}+ip_{y0} = p^+|_{z=0}$ is the initial value. Below the two limiting cases are discussed.

(1) $L_0 \gg \lambda_0$, in which $\lambda_0 = 2\pi/k_0$ is the wave length of the fluctuator and at this time $B_w(z)$ is slowly increasing. Formula (4) can be approximated as

$$p^+ = p_0^+ - \frac{eB_w(z)}{ck_0}e^{ik_0 z} \tag{5}$$

or written as

$$p_x = p_{x0} - \frac{eB_w(z)}{ck_0}\cos k_0 z,$$

$$p_y = p_{y0} - \frac{eB_w(z)}{ck_0}\sin k_0 z_\circ \tag{6}$$

when $B_w(z)$ varies slowly, the vector potential of the fluctuation field $A_w = -B_w/k_0$ and the transverse regular momentum $P_\perp = P_\perp + eB_w(z)/ck_0$. It is easy to see that the transverse regular momentum represented by formula (6) is constant. That is to say, when the variation of the fluctuation field is very slow, the transverse regular momentum is adiabatically invariant.

(2) $L_0 \to 0$, This means at z=0 the fluctuation field has a mutation. At this time formula (4) tends to

$$p^+ = p_0^+ = \frac{eB_{w0}}{ck_0}(e^{ik_0 z} - 1) \tag{7}$$

or, written in component form

$$p_x = p_{x0} - \frac{eB_{w0}}{ck_0}(\cos k_0 z - 1),$$

$$p_y = p_{y0} - \frac{eB_{w0}}{ck_0}\sin k_0 z_\circ \tag{8}$$

It is evident that the x component of regular momentum before and after entering the fluctuation field is no longer conserved and a discontinuity eB_{w0}/ck_0 appears. P_x does a cosine variation about the average value $\bar{p}_x = p_{x0} + eB_{w0}/ck_0$ The sort of mutation discussed here is the limiting case of non-adiabatic injection.

Usually $|p_0^+|$ is very small and can be ignored. From formula (6) we see that with respect to adiabatic injection, the transverse momentum of the electrons after injection into the interaction zone, $p_\perp \cong eB_{w0}/ck_0 =$ a constant. Since p is a constant P_z is a constant. This sort of non-orbiting is what is needed. For conditions of non-adiabatic injection, from formula (8) ignoring P_x0 and P_y0, we can get

$$p_\perp = 2(eB_{w0}/ck_0)\,|\sin(k_0 z/2)|,$$

further we can get

$$p_z \cong p - \frac{2}{p}\left(\frac{eB_{w0}}{ck_0}\right)^2 \sin^2\frac{k_0 z}{2} \tag{9}$$

Here we have supposed that $eB_{w0}/ck_0 << p$. It is evident that for this sort of non-adiabatic injection situation, P_z produces a component which fluctuates with position. Longitudinal velocity fluctuation with position is not desirable since it can lead to degrading the laser performance as in increasing the band width and lowering the gain. This sort of fluctuation of the longitudinal momentum can be equivalent to a momentum component dispersion degree

$$\left(\frac{\Delta p_z}{p_z}\right)_{e.v} \cong 2\left(\frac{eB_{w0}}{ck_0}\right)^2 / p^2 \tag{10}$$

Usually $eB_{w0}/ck_0 \sim (0.1 \sim 0.2)p$, 因此 $(\Delta p_z/p_z)_{e.v} \sim (2 \sim 8)\%$。 It is necessary to point out that the non-adiabatic injection discussed here is a limiting condition where $B_w(z)$ is a step function. For non-adiabatic injection where $B_w(z)$ is continuously varying, the corresponding $(\Delta p_z/p_z)_{e.v}$ is smaller than the value obtained here.

In the use of free electron lasers with high density electron beams, generally we must add an axial magnetic field. Because there is strong coupling between the electron revolving around the axial magnetic field and moving in the fluctuation field, the variations in velocity are very complex. In the treatment below we assume that the transition zone of the axial magnetic field and the transition zone of the fluctuation field are separate and can be considered individually.

Figure 1 shows a normally used experimental design[1]. The graph in the lower part of the figure represents the variation of the axial magnetic field along the longitudinal direction, the special feature of which is that the magnetic field at the output of the accelerator is rather strong, being about twice the interaction zone magnetic field. The figure is the situation of an oscillator. M_1 and M_2 are mirrors and the broken line stands for the outline of the electron beam.

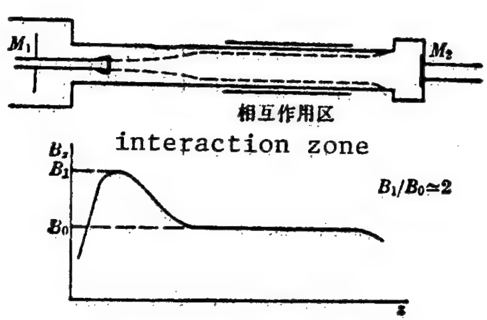

Fig. 1 Experimental Design of a Free-Electron Laser Oscillator with an Axial Magnetic Field and the Distribution of the Magnetic Field along the Longitudinal Direction

Because the axial magnetic field is rather strong, the rotation radius of the electrons is very small and magnetic moment conservation can be considered satisfied, i.e. $T_\perp = B_z$ = a constant, $T_\perp$ representing the electron's transverse temperature. The gradual reduction in the axial magnetic field leads to gradual cooling of the transverse temperature because this sort of initial transverse temperature is not at all necessary. For high density electron beams, in order to reduce the influence of spatial charge effects, frequently an annular beam is used rather than a solid beam. When using the above magnetic field position style, one makes the feedback route of the light rays avoid the cathode. This point is necessary for oscillators.

Below we discuss the motion of the electron beam in the transition zone. Suppose that the axial field has already entered the homogeneous section, as shown in Fig. 1 by B_0. At this time the total magnetic field can be written as

$$\boldsymbol{B} = B_0\hat{e}_z + B_w(z)(\hat{e}_x \cos k_0 z + \hat{e}_y \sin k_0 z) \tag{11}$$

while the electron motion equations are still described by formula (2). Since there is present only a stable magnetic field, similarly we can deduce that p = a constant, and consequently the relativity factor γ = a constant. Substituting in rotational coordinates

$$\begin{aligned} \hat{e}_1 &= \hat{e}_x \cos k_0 z + \hat{e}_y \sin k_0 z, \\ \hat{e}_2 &= -\hat{e}_x \sin k_0 z + \hat{e}_y \cos k_0 z \end{aligned} \tag{12}$$

Then equation (2) can be written in component form

$$\begin{aligned} \frac{dv_1}{dt} &= v_2(k_0 v_z - \omega_o), \\ \frac{dv_2}{dt} &= -\omega_w v_z - v_1(k_0 v_z - \omega_o), \\ \frac{dv_z}{dt} &= \omega_w v_2, \end{aligned} \tag{13}$$

in which $\omega_o = eB_0/m\gamma c$, $\omega_w = eB_w(z)/m\gamma c$.

If $B_w(z)$ = a constant, then the equations (13) have two integration constants:

$v = (v_1^2 + v_2^2 + v_z^2)^{1/2}$, $\theta = \eta^2 - 2\varepsilon v_1 k_0/\omega_o$, in which $\varepsilon = B_w/B_0$, $\eta = (k_0 v_z/\omega_o - 1)$

is the normalized longitudinal velocity. In what follows we discuss only the situation where $B_w(z)$ adiabatically varies. At this time the integration constant θ can be considered approximately established. Using the integration constants v and θ we can eliminate v_1 and v_2 from equations (13) getting an equation that only contains v_z

$$\left(\frac{d\eta}{d\tau}\right)^2+\eta^4+4\left(\varepsilon^2-\frac{\theta}{2}\right)\eta^2 \qquad +8\varepsilon^2\eta+4\varepsilon^2(1-\lambda^2)+\theta^2=0 \tag{14}$$

in which $\lambda^2=v^2k_0^2/\omega_c^2$, $\tau=\omega_c t/2$ is the normalized time interval, differentiating once with respect to τ gives

$$\frac{d^2\eta}{d\tau^2}+2\eta^3+4\left(\varepsilon^2-\frac{\theta}{2}\right)\eta+4\varepsilon^2=0 \tag{15}$$

This is a Duffing equation without a driving term. The equation derived here is substantially the same as the one arrived at by Mcmullin and Davidson.[2] It is difficult to solve equation (15) for a rigorous analytical solution, but usually the fluctuation field amplitude η is very small so we can linearize the fluctuation equilibrium point η_0 about which η changes in equation (15). The concrete steps can be referred to in reference [2]. Here we only give the result

$$v_z=V_b+\delta V_b\cos(\omega_\delta t+\alpha_0) \tag{16}$$

When $\theta\cong 0$ 时, $\omega_\delta=(3/2)^{1/2}2^{1/3}\varepsilon^{2/3}\omega_c$, $V_b=\frac{\omega_c}{k_0} \times(1-2^{1/3}\varepsilon^{2/3})$。 . And δV_b is determined by the following formula

$$\delta V_b=\left\{(v_{z0}-V_b)^2 \quad +\left[\varepsilon\frac{\omega_c}{k_0}\,\frac{k_0v_{\perp 0}}{\omega_\delta}\sin(k_0z_0-\phi_0)\right]^2\right\}^{\frac{1}{2}} \tag{17}$$

in which v_{z0}, $v_{\perp 0}$, and z_0 represent the corresponding initial values and ϕ_0 is the angle between $v_{\perp 0}$ and $\hat{e}_x$. Obviously the maximum value of δV_b is

$$\delta V_{bmax}=\left[(v_{z0}-V_b)^2 \quad +\left(\varepsilon\frac{\omega_c}{k_0}\,\frac{k_0v_{\perp 0}}{\omega_\delta}\right)^2\right]^{\frac{1}{2}} \tag{18}$$

δV_{bmax} represents the fluctuation amplitude of v_z which is composed of two parts. One part is created because the initial longitudinal velocity v_{z0} and the equilibrium point V_b of the fluctuation are not the same. With suitable selection of system parameters, the contribution of this part can be made very small. The other part comes from $v_{\perp 0}$. That is to say, after passing through the transition zone, $v_{\perp 0}$ can induce a fluctuation in the longitudinal velocity. For this reason we desire $v_{\perp 0}$ to be as small as possible. This is why we adopted the position style of an axial magnetic field shown in Fig. 1 to cool the transverse temperature of the electrons.

The above analysis was done for conditions where $\theta \cong 0$. When this condition is not satisfied, the form of representation of V_b and $\omega\delta$ also change correspondingly. But it is conceivable that the above discussion has generality.

If the variations of the transition zone fluctuation field are faster, the adiabatic approximation not longer stands, and the fluctuation of the induced v_z will be even larger. This is because a more rapidly varying fluctuation field introduces a larger transverse velocity which is equivalent to an increase in the initial transverse velocity. For this reason also adiabatic injection is desirable.

III. Further Analysis of the Longitudinal Energy Dispersion

Longitudinal energy dispersion, longitudinal momentum dispersion, and longitudinal velocity dispersion are used in this paper with a equivalent meaning. Taking the general meaning, it refers to the non-singularity of the electron beam's longitudinal energy within the range of the interaction zone and interaction time. We have already pointed out that this index is an extremely important parameter to measure the quality of the electron beam. This is because dispersion of the longitudinal energy will too greatly lower the gain and efficiency leading to increase of the beam width, degrading the performance of the laser.

Apart from periodic fluctuation of longitudinal velocity according to position caused by a non-adiabatically injected electron beam which we have discussed above, and the longitudinal velocity fluctuations caused by coupling between the motion revolving about the axial magnetic field and the motion within the fluctuation field when there are conditions with an axial magnetic field, the limited emissivity of the electron beam, the spatial charge effects of a high density electron beam, the presence of a transverse gradient in the fluctuation field, and time variations of accelerator potential all can influence the magnitude of the longitudinal energy dispersion. The features of the dispersion caused by these factors are by no means entirely the same. We can divide them into the following categories.

1. Electron beam longitudinal energy dispersion at a given time and place. The longitudinal energy dispersion caused by limited emissivity belongs to this type. The definition of emissivity is $\varepsilon = \pi R \langle \theta^2 \rangle^{\frac{1}{2}}$, in which R is the beam radius, $\langle \theta^2 \rangle^{1/2}$ is the γ.m.s value of the angle between the electron orbit and the axis. Clearly, even if the electron beam is monenergetic, since $\varepsilon \neq 0$, a dispersion will appear in the longitudinal velocity. If ε is very small, it is easy to derive the dispersion

$$\frac{\Delta v_z}{v_z} = \frac{\varepsilon^2}{2\pi^2 R^2} \tag{19}$$

Supposing the laser efficiency to be η, to make it so that stimulated Raman scattering can be produced requires $\Delta v_z / v_z \ll \eta / \gamma_{z0}^2$.

2. Positional variations of the electron beam longitudinal energy at a given time. This can be further subdivided into variations according to transverse position and variations according to longitudinal position. The longitudinal velocity fluctuation caused by non-adiabatic injection is an example of longitudinal positional variation. The self potential produced by space charge effects leads to variations of the longitudinal velocity according

to transverse position, which is what is commonly called the shearing of longitudinal velocity present along the radial direction. It is easy to derive for a solid electron beam the electric potential difference across the beam radius $\Delta V=I/4\pi\varepsilon_0 z_z$ (MSKA units), I is the total current. Supposing the total energy is fixed, then the electric potential, according to the variation in transverse position, will cause longitudinal energy shearing along the radial direction. Letting the equivalent accelerator voltage of the accelerator be V, then we desire $\Delta V/V<<\eta$. For an annular electron beam, let a be the ring radius and t be the ring thickness, then

$$\Delta V=(I/4\pi\varepsilon_0 v_z)(t/a)_\circ$$

Since t<<a, when the total current is fixed, the potential difference of this electron beam across the radius is far less than for a solid electron beam. In other words, after the permitted upper bound of $\Delta V/V$ is given, the permitted current is larger. This is why high density electron beam experiments mostly use annular beams.

For physically achievable fluctuation fields, inside the cavity of the interaction zone, they must satisfy the condition $\nabla.B=\nabla XB=0$. Consequently it cannot be homogeneous along the transverse direction. This sort of transverse gradient in the fluctuation field can also cause longitudinal velocity shearing, but it also has a reducing effect on the shearing caused by spatial charge effects.

3. Time variations in the electron beam longitudinal energy at a given position. Time variations of the accelerator voltage can cause this sort of effect. Letting the variation in accelerator voltage be δV and desiring stimulated Raman scattering then we want $\delta V/V<<\eta$.

REFERENCES

1. Birkett, D.S. et al., IEEE J. Quant. Electr., 1981, QE-17, 1348.

2. Mcmullin, W.A. and R.C. Davidson, Phys. Rev. A, 1982, 25, 3130.

12966/7358
CSO: 4008/22

XeCl EXCIMER LASER WITH MAGNETIC COMPRESSOR

Shanghai ZHONGGUO JIGUANG [CHINESE JOURNAL OF LASERS] in Chinese Vol 13, No 11, 20 Nov 86 pp 683-686

[Article by Lou Qihong [1869 4388 3163], Qi Jianping [4349 1696 1627], Wang Runwen [3769 3387 2429], Wei Yunrong [7614 6663 2837], Ding Aizhen [0002 1947 5271], Dong Jingxing [5516 2529 2502], Ding Zean [0002 3419 1344], Wu Guoqing [0702 0948 1987] of the Shanghai Institute of Optics and Fine Mechanics, Chinese Academy of Sciences; manuscript received 3 Aug 85]

[Text] Abstract: This paper studies the characteristics of adopting an excimer laser with a magnetic compressor. Using this kind of technique the current pulse rise time can be compressed from 200 ns to 50 ns. We compute the current pulse amplification and compression phenomena, explain the reason for reduction of back current amplitude, and provide the effects of bypass inductance on the compression results.

I. Introduction

The addition of a magnetic saturation coil to the discharge circuit is considered one of the key techniques for increasing the repetition frequency and operating life of excimer lasers.[1] When the current flowing through the magnetic saturation coil is smaller it has a larger inductance and the change in resistance to current flow causes the circuit to be in a closed state. When the current increases to a certain value, the magnetic material of the magnetic permeability tends to 1, and the induction suddenly becomes small. The result of this is to make a sudden change appear in the circuit current. Consequently the circuit is characterized by compressed pulses thus it is called a magnetic compressor.

Through the speed change of the magnetic compressor, an electrical pulse has a very short rise time. This is beneficial for forming large volume homogeneous pulsed avalanche discharge. In addition, it allows the switch components used before the magnetic compressor to operate with a wider pulse width consequently receiving a smaller current and current change dI/dt.[2] Whether for thratrons or spherical gaps, this can vastly prolong their useful life.

This paper analyzes theoretically the compression results of the pulse current after using a magnetic compressor. In experimental designs we made a magnetic

saturation coil and applied it in an X-ray pre-ion laser and observed the current pulse width to be compressed from 200 ns to 50 ns. In order to design an optimal circuit, we also studied the effect of by-pass induction on the compression results.

II. Theoretical Analysis

In Fig. 1, (a) shows the capacitor transfer discharge circuit used in general experiments. Capacitor C_1 charges from the direct current source up to V_0. After the switching component K conducts, the electrical energy on C_1 transfers to C_2 and shortly the voltage on C_2 exceeds the breakdown value of the laser. In our experiments we added the magnetic saturation coil L_m. The equivalent circuit of Fig.1 (a) is given in Fig. 1(b) in which L_k is the distributed inductance in the circuit of the switch K after it conducts and R is distributed resistance of K after it conducts.

Fig. 1

(a) Laser Discharge Circuit using a Magnetic Compressor

(b) Equivalent Circuit

$(C_1=27\,\text{nF};\ C_2=18\,\text{nF};\ L_3=8\,\mu\text{H};\ R=0.5\,\Omega)$

For describing the charging process of C_2 we can use the following differential equation

$$\begin{cases} L\dfrac{di}{dt}+Ri+\left(\dfrac{1}{C_1}+\dfrac{1}{C_2}\right)\displaystyle\int i\,dt=0; \\ i\,|_{t=0}=0; \\ V_{C_2}|_{t=0}=-V_0 \end{cases} \qquad (1)$$

In the formula $L=L_k+L_m$; L_m is the inductance of the magnetic saturation coil. Make

$$C=C_1C_2/(C_1+C_2);$$

$$b=R/2L;$$

$$\omega=\left(\frac{1}{LC}-\frac{R^2}{4L^2}\right)^{1/2};$$

and we can represent the time variation of the current, i, as

$$i = -\frac{V_0 C_1}{\omega LC} e^{-bt} \sin(\omega t) \tag{2}$$

If di/dt=0, $|i|$ reaches a maximum value. At this time we can get the time, t_0 when the current reaches the maximum value:

$$\begin{aligned} t_0 &= \frac{1}{\omega}\, tg^{-1} \frac{\omega}{b} \\ &= \frac{1}{\omega}\, tg^{-1}\left(\frac{4L}{R^2 C} - 1\right)^{1/2} \end{aligned} \tag{3}$$

The voltage V_{C_2} on the capacitor C_2 can be expressed as

$$V_{C_2} = \frac{V_0 C_1}{C_1 + C_2} \left[1 - \frac{1}{\omega\sqrt{LC}} e^{-bt} \sin(\omega t + \varphi)\right]; \tag{4}$$

in which $\phi = \tan^{-1}(w/b)$.

From formula (4) we can also get the voltage rise time t_1

$$t_1 = \frac{2\pi}{\omega} = \frac{2\pi}{\sqrt{\frac{1}{LC} - b^2}}; \tag{5}$$

When the magnetic saturation coil is not present, $L=L_k$ and the current wave form computed from equation (2) is shown by the dashed line in top part of Fig. 2. The parameters used in the computation are given in the note to the figure. When the magnetic saturation coil is present, since the non-saturated inductance of L_m is very large, the circuit current is very small. After an interval Δt, the inductor's magnetic core saturates quickly, $\mu \to 1$, and the current changes suddenly. Under the conditions of this paper $\Delta t \sim 100$ ns. Consequently in the computation of the current wave form there appears a narrower current pulse. However, the above model does not yet truly reflect the characteristics after magnetic saturation because the inductance L_m was large before the magnetic saturation coil was saturated, storing a portion of the electrical energy. The change in current made the saturation coil produce a corresponding induced electromotive force V_m. According to the magnetic saturation inductance formula[3,4]

$$\begin{aligned} \phi &= \int V\, dt = NA\Delta B \\ V_m &= \frac{\phi}{T_{sat}} = \frac{\int_0^{T_{sat}} V \cdot dt}{T_{sat}} = \frac{NA\Delta B}{T_{sat}} \end{aligned} \tag{6}$$

in which N is the number of inductance turns of the magnetic saturation coil; A is the cross section of the magnetic material; ΔB is the magnetic saturation density of the magnetic material; and T_{sat} is the time necessary for the material to reach a magnetic saturation state. Consequently when the magnetic saturation coil quickly saturates, the voltage in the circuit ought to be the sum of the voltage V_1 across C_1 and the EMF V_m induced across the magnetic saturation coil. Based on the above analysis we can get the current wave form after the magnetic saturation coil is present in the circuit:

$$\begin{cases} i(t) = -\dfrac{V_0 C_1}{\omega(L_k+L_m)C} e^{-bt}\sin(\omega t), t \leq \Delta t \\ i(t) = -\dfrac{(V_0+V_m)C_1}{\omega' L_k C} e^{-b't}\sin(\omega' t), t > \Delta t \end{cases} \tag{7}$$

in which $\omega=\left(\dfrac{1}{(L_k+L_m)C}-\dfrac{R^2}{4(L_k+L_m)^2}\right)^{1/2}$; $\omega'=\left(\dfrac{1}{L_k C}-\dfrac{R^2}{4L_k^2}\right)$; $b=R/2(L_k+L_m)$; $b'=R/2L_k$.

The current wave form calculated based on formula (7) is shown by the dashed line in the bottom half of Fig. 2. Of note is that the saturation interval of the saturation inductance is very short. After the post saturation current reaches its maximum value, the current changes from big to little reversing the polarity of the induced EMF V_m of the saturation inductor and the voltage V_0 of the capacitor C_1. The result is that the back current amplitude is reduced, a feature which is of great advantage for repetition frequency operation.

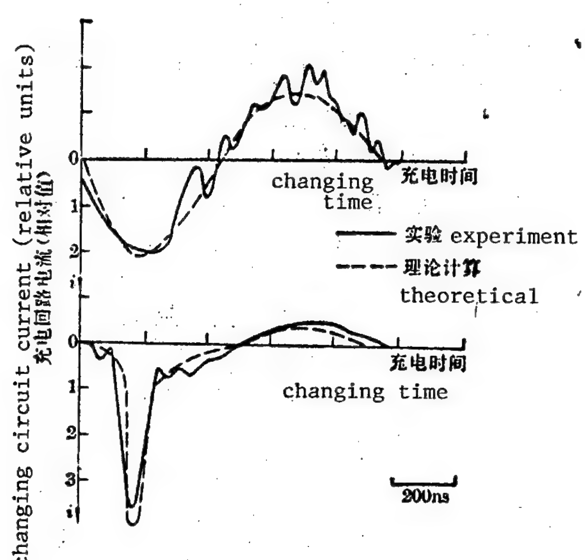

Fig. 2 Effect of a Magnetic Saturation Coil on Current Wave Form

(Above) Without the magnetic saturation coil

(Below) With a magnetic saturation coil

III. Experimental Results and Discussion

The laser used in the experiments was a capacitor transfer style discharge circuit pumped, X-ray pre-ion XeCl excimer laser. The magnetic saturation coil used a rectangular magnetic stamen of metallic glass with wrapped wire. The outer dimensions were 5 cm X 5 cm X 60 cm and the cross section of the magnetic stamen was 25 cm^2.

The laser discharge volume was about 2 X 2 X 60 cm^3 and used a parallel plate structure as a resonance cavity. The laser energy was measured by a (tan dou ke ji cha ce). A (ru ke fu si ji) coil was used to measure the change over time of the current in the charging circuit. We measured the coil up against the magnetic compressor at point A in Fig. 1(a). Under conditions without the magnetic saturation coil, the current wave form was approximately a normal sine curve (See the solid line in the top half of Fig. 2) which agrees well with our theoretical results of the previous section. Note that the current wave form for the second half period is not as smooth as in the first half. This is mainly because after discharge the pre-ion action is not present and the discharge produces streamer shaped spikes. When the magnetic saturation coil is introduced into the circuit, the current wave form is like that shown by the solid line in the lower part of Fig. 2 and shows clearly the narrowing of the current pulse and the reduction in back current. This wave form is identical to the computations of the theoretical model.

In order to obtain the desired compression ratio, one must first match up the charging time of C_1 and C_2 with the saturation time Δt of the magnetic saturation coil. Since after working the dimensions of the selected material for the magnetic saturation coil Δt is fixed, and the values of C_1 and C_2 in the laser are also fixed, general analysis gives the charging time constant of C_2 as

$$T_C = \pi (L_3 C_2/2)^{1/2} \tag{8}$$

Superficially it seems that the deficiency between the two can be matched by adjusting parameters. Actually, the T_C given by formula (8) is related to the by-pass inductance L_3 and only when the value of L_3 is large and its high frequency impedance far exceeds the high frequency impedance of C_2 can formula (8) be used to compute T_C. Consequently, we can do matching by adjusting the size of L_3. When L_3 is too small, its high frequency impedance no longer exceeds that of C_2, making the charging time, T_C, be too small. The result is that the magnetic saturation coil is unable to reach the proper saturation value thereby effecting the compression results. On the other hand, when L_3 is too large, it will make the charging time of C_2 be longer with the result that the saturation process is slowed. Figure 3 is the observed pulse discharge current width (FWHM) and corresponding change in laser output energy for L_3 from 1 μH to 16 μH. These experimental results verify our analysis above. A suitable selection of L_3 can make T_C and Δt match up to obtain optimal magnetic compression results. At this time τ will be a minimum and the laser output energy, E, will be maximum.

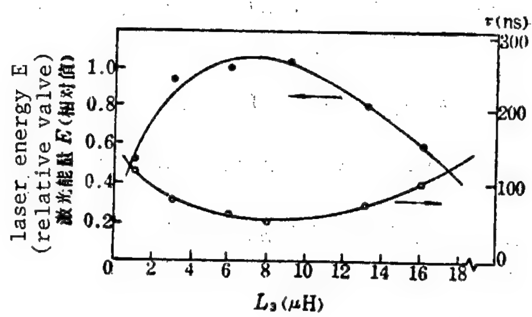

Fig. 3 Effect of the By-pass Inductance L_3 on the Magnetic Saturation Coil Compression Results and on the Laser Output Energy

Figure 4 shows the laser operating characteristics after using a magnetic saturation coil. The transverse coordinate is time delay between laser discharge and X-ray pre-ions. For comparison, the figure also gives the characteristics without a magnetic saturation coil. From the figure we can see that after the introduction of a magnetic saturation coil the variation of laser output versus delay is more sensitive than before. However, since the magnetic saturation coil itself has some dissipation and will dissipate a part of the energy this makes the energy output of the laser fall a bit but if one just selects a suitable time delay the dissipation caused by the magnetic saturation coil can be kept to about 10 percent. A compensation for the cost of this dissipation is that the life of switching components in a laser apparatus with a magnetic compressor will be prolonged by an order of magnitude. As for spherical gap switches, this arrangement can stretch out the time between cleaning and repairs. For a thyratron, it can prolong the operating life even more.

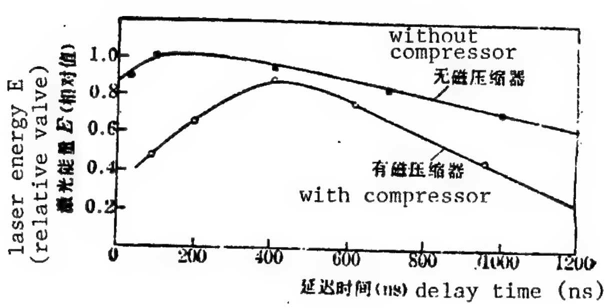

Fig. 4 Effect of a Magnetic Saturation Coil on Laser Output Energy

REFERENCES

1. K. Noda et al., "CLEO'85 Technical Digest," 21-24 May 1985, Baltimore MD USA, Paper WM-26, p. 118.

2. I. Smilanski et al., APP. PHYS. LETT., 1982, 40, No. 7, 547.

3. D. Bazting et al., LASER UND OPTOELEKTRONIK, 1982, No. 2, 128.

4. M. Stockton et al., J. APPL. PHYS., 1982, 53, No. 3, 2765.

12966/7358
CSO: 4008/22

TWO IMPROVED METHODS OF SPECTRAL FACTORIZATION

Beijing QINGHUA DAXUE XUEBAO (ZIRAN KEXUE BAN) [JOURNAL OF QINGHUA UNIVERSITY (NATURAL SCIENCE)] in Chinese Vol 26 No 6, Dec 86 pp 9-16

[English abstract of article by Li Yanda [2621 5888 6671], et al., of the Department of Automation]

[Text] When the zeroes of a signal are very close to the unit circle in the Z-plane, using Kolmogoroff's method will cause a large error. An improved method is proposed in this paper. The error from Kolmogoroff's method can be detected and reduced by this method. Based on an iterative method proposed by T.F. Quatieri et al., the authors suggest an improved method in which s(0) is not necessary. Therefore, the improved method can be used over a wide range. Some examples are given. (Paper received October 1985.)

REFERENCES

[1] J.F. 克利尔波特：《地球物理数据处理基础》，石油出版社，1976 年
[2] T. F. Quatieri, A. V. Oppenheim, **IEEE. Trans.**, ASSP-29, 6(1981), 1187—1193
[3] M. H. Hayes, **IEEE. Trans.**, ASSP-30, 2(1982), 140—154
[4] V. T. Tom, T. F. Quatieri, M. H. Hayes, J. H. McClellan, **IEEE. Trans.**, ASSP-29, 5(1981), 1052—1058
[5] A.V.奥本哈姆，R.W.谢弗：《数字信号处理》，科学出版社，1982 年

CSO: 4009/1083

CONVERGENCE AND CONTROL MAGNITUDE OF THE SELF-TUNING REGULATOR

Beijing QINGHUA DAXUE XUEBAO (ZIRAN KEXUE BAN) [JOURNAL OF QINGHUA UNIVERSITY] (NATURAL SCIENCE)] in Chinese Vol 26 No 6, Dec 86 pp 29-37

[English abstract of article by Li Qingquan [2621 3237 3123] of the Department of Automation]

[Text] The general representations of the self-tuning regulator are given. The relationships between the regular parameters and the convergency and control action are analyzed. A new limitation-convergence combined control strategy is presented. The strategy covers both requirements of the control magnitude and convergence rate well. Experimental results are given. (Paper received October 1985.)

REFERENCES

[1] Harris, C. J., and S. A. Billings (Eds.), **Self-tuning and Adaptive Control: Theory and Applications**, Peter Peregrinus, London, 1981

[2] 应书光，《自动化学报》，6，2(1980)，85—93

[3] Åström K. J., and B. Wittenmark, **Automatica**, 9(1973), 185—199

CSO: 4009/1083

QUESTION USING STEADY-STATE MODEL TO CALCULATE WATER QUALITY IN TIDAL RIVER

Beijing QINGHUA DAXUE XUEBAO (ZIRAN KEXUE BAN) [JOURNAL OF QINGHUA UNIVERSITY (NATURAL SCIENCE)] in Chinese Vol 26 No 6, Dec 86 pp 38-47

[English abstract of article by Li Yuliang [2621 3768 2856], et al., of the Department of Hydraulic Engineering]

[Text] The dynamic model of water quality was averaged over a tidal period and the results obtained were compared with those of the steady-state model. Equivalent conditions of the two sets of equations were found theoretically. Two conditions were proposed which should be satisfied when using the steady-state model in the tidal river. Tidal acceleration in the river which will influence the calculation reliability of the steady-state model is introduced and determined. The expression for estimating the effect of the changing tidal acceleration on the water quality calculation parameter is established. An analytical method computing pollutant concentration in the tidal river using the steady-state model is proposed. (Paper received December 1985.)

REFERENCES

[1] G. T. Orlob: **Mathematical Modeling of Water Quality: Streams, Lakes and Reservoirs,** John Wiley & Sons Inc., 1983, 215.

[2] С. Э.Фриш 及 А. В. Тиморева 著：《普通物理学》，梁宝宏译，高等教育出版社，1954，417。

[3] 清华大学土木与环境工程系及环境系统工程研究室：《水污染控制系统规划》，清华大学出版社，1982。

[4] R. L. Crim & N. L. Lovelace: **Auto-Qual Modelling system,** U. S. Environmenal Protection Agency, Office of Air and Water Programs, Washington D. C., 1973.

CSO: 4009/1083

STRUCTURAL INVESTIGATION OF FLUORIDE-BEARING LIQUID CRYSTAL OF MB80.5 (F) BY X-RAY DIFFRACTION

Beijing QINGHUA DAXUE XUEBAO (ZIRAN KEXUE BAN) [JOURNAL OF QINGHUA UNIVERSITY (NATURAL SCIENCE)] in Chinese Vol 26 No 6, Dec 86 pp 48-56

[English abstract of article by Wang Xinjiu [3769 2450 0036] of the Department of Modern Applied Physics; A.J. Leadbetter and G. Etherington of Rutherford Appleton Laboratory, SERC, United Kingdom]

[Text] The fluoride-bearing organic compound (MB80.5 (F)) exhibits more complex liquid crystal phases. Its phases and phase transition temperatures have been determined by the X-ray diffraction technique with two-dimensional multiwire position-sensitive detectors for the single domain of the sample. The temperature dependencies of the apparent molecular lengths and the distances of neighboring molecules of all the phases, the smectic layer thicknesses of three smectic phases S_A, S_C and S_F, as well as the tilt angles of the molecules in the layers of the S_C phase, have also been measured. (Paper received March 1986.)

REFERENCES

[1] 王新久、陶琨、赵静安，《清华大学学报》，25，4(1985)，41

[2] Eheringto G., Leadbetter A. J., Wang X. J., Gray G. W., Tajbakhsh A., **Liquid Crystals**, 1(1986), 209

[3] Leadbetter A. J., **The Molecular Physics of Liquid Crystals**, Ed, Luckhurst G. R., Gray G. W., Academic Press, N. Y., 1979, 285—316; Doucet, J., ibid, 317—342

[4] Bateman J. E., et al, **Nucl. Instr and Meth.**, 217(1983), 77; Bateman J. E., **Nucl. Instr. and Meth.**, 221(1984), 131

[5] Ed. Weast R. C., Astle M. J., **Handbook of Chemistry and Physics**, 63rd edition, CRC Press, Boca Raton, Florida, 1982, 180—184

[6] Leadbetter A. J., Wrighton P. G., **J. de Physique**, 40(1979), C3—234

[7] James R. W., **The Optical Principles of the Diffraction of X-Rays**, G. Bell and Sons, London, 1954, 513—589

CSO: 4009/1083

DETERMINATION OF n, k, d VALUES OF ABSORBING THIN FILMS USING MULTI-INCIDENT ANGLE ELLIPSOMETRY TECHNIQUE

Beijing QINGHUA DAXUE XUEBAO (ZIRAN KEXUE BAN) [JOURNAL OF QINGHUA UNIVERSITY (NATURAL SCIENCE)] in Chinese Vol 26 No 6, Dec 86 pp 67-75

[English abstract of article by Wei Zhiyuan [7614 1807 3220], et al., of the Department of Radio Electronics]

[Text] This paper presents a non-destructive n, k, d value determination of absorbing thin films, i.e., the QWD-84 method, using a multi-incident angle ellipsometry technique. A few important aspects have been investigated during the determination. Some absorbing thin films on glass and monocrystalline silicon substrates have been measured. Good agreement is obtained between the QWD-84 method and the spectrophotometer results as well as step height measurements. The results indicate that QWD-84 is feasible, effective, undamaged and reliable for determining the n, k, d values of absorbing thin films. (Paper received September 1985.)

REFERENCES

[1] 吴启宏，唐晋发，《浙江大学学报》，4(1980)，89

[2] 冯浩善，《陕西电子》，2(1979)，10

[3] 莫党、朱雅新，《物理》，6，3(1977)，140

[4] 吴启宏，《北京光学》，2～3 (1981)，5

[5] 杨明芳，《光学工程》，4(1984)，15

[6] C. L. Nagendra, Vacaum, 31, 3(1981), 141

[7] C. M. Horwitz, Applied Optics, 17, 11(1978), 1771

[8] 严樟根、魏志渊、周邦伟，《中国真空学会第二届年会论文集》，2,(1983),246

[9] 严樟根、殷志强、魏志渊、周邦伟，《真空科学与技术》，1(1986)，57

[10] 南京大学数学系编：《最优化方法》，科学出版社，1978

[11] 郑权、蒋百川、庄松林，《应用数学学报》，1，2(1978)，161

[12] 郑权、唐晋发、蒋百川，《浙江大学学报》，1 (1980)，1

CSO: 4009/1083

LOCALLY ANALYTICAL DIFFERENCE SCHEME AND ITS APPROXIMATE DIFFERENCE SCHEMES FOR CONVECTION DIFFUSION EQUATION

Beijing QINGHUA DAXUE XUEBAO (ZIRAN KEXUE BAN) [JOURNAL OF QINGHUA UNIVERSITY (NATURAL SCIENCE)] in Chinese Vol 26 No 6, Dec 86 pp 76-85

[English abstract of article by Lu Jinfu [7120 6855 3940], et al., of the Department of Applied Mathematics]

[Text] In this paper, some approximate difference schemes of locally analytical difference schemes for an approximate solution of the convection-diffusion equation are derived and the method for constructing such difference schemes and the relationship between them are given. The stability conditions, suitability for convection-dominated problems and other properties of these difference schemes are discussed. Numerical results and analysis show that the Samarsky scheme is the optimal one. (Paper received March 1986.)

REFERENCES

[1] R. L. Roach, AIAA Paper No. 82—0102 (1982)

[2] 黄铎, 《计算数学》, 5, 5 (1983)

[3] S. C. R. Dennis, D. B. Ingham and R N. Cook, **J. Computational Phys.**, 33 (1979), 325—339

[4] M. M. Gupta, **Int. J. Numer. Methods fluids**, 3(1983), 319—331

[5] A. C. Hindmarsh, P. M. Gresho and D. F. Griffiths, **Int. J. Numer Methods fluids**, 4(1984), 853—897

[6] E. F. Nogotov, **Applications of Numerical Heat Transfer**, Unesco., Paris, 1978

[7] 黄铎, 《计算物理》, 2, 2 (1985), 161—166

[8] J. Noye, **Computational techniques for differential equations**, North-Holland Publishing Coy., Amsterdam, 1984

[9] B. P. Leonard, **Comp. Methods in Applied Mech. and Eng.**, 19(1979), 59—98

[10] M. K. Patel, N. C. Markatos and M. Cross, **Int. J. Numer. Methods fluids**, 5(1985), 225—244

CSO: 4009/1083

EFFECT OF TENSILE RESIDUAL STRESSES ON FATIGUE FAILURE OF ROLLING-SLIDING CONTACT

Beijing QINGHUA DAXUE XUEBAO (ZIRAN KEXUE BAN) [JOURNAL OF QINGHUA UNIVERSITY (NATURAL SCIENCE)] in Chinese Vol 26 No 6, Dec 86 pp 86-94

[English abstract of article by Zhang Jun [1728 6511], et al., of the Department of Precision Instruments and Mechanology]

[Text] An experimental investigation has been made to determine the effect of residual stresses on fatigue life of rolling-sliding contact. The results show that the tensile residual stress is detrimental to fatigue properties of the roller. The accurate calculation of the stress field based on EHL theory and the theory of elasticity shows that the shear stresses at the surface in the direction of 30° with rolling direction cause the pitting cracks and the tensile stresses accelerate the crack growth. (Paper received December 1985.)

REFERENCES

[1] Smith J. U., Liu C. K., **Journal of Applied Mechanics**, 20, (1953), 157—166

[2] Czyzewski T., **Wear**, 31, 1(1975), 119

[3] 徐秉业等：《弹塑性力学》，清华大学出版社，1983。

9717
CSO: 4009/1083

DEVELOPMENT AND APPLICATION OF β-TYPE CRYSTAL POLYPROPYLENE RESIN

Lanzhou HECHENG XIANGJIAO GONGYE [SYNTHETIC RUBBER INDUSTRY] in Chinese
Vol 10 No 1, Jan 87 pp 8-12

[English abstract of article by Li Zhongyao [2621 0112 1031], et al., of the Chemical Engineering Research Institute, Lanzhou Chemical Industry Corporation; Shi Guanyi [0670 6034 0001], et al., of Shanghai Institute of Organic Chemistry, Chinese Academy of Sciences]

[Text] The β-type crystal polypropylene resin with high content of β-type crystal polypropylene was developed by re-granulation with α-type crystal polypropylene together with added nucleator complex LS-CXA through an extruder. The results show that under the laboratory's experimental conditions, the β-type crystal polypropylene content in the product obtained by this method from homopolymers of propylene can reach as high as 85-95 percent. LS-CXA to the homopolymer of propylene is 0.1 parts per hundred parts of polypropylene (mass ratio), the content of β-type crystal polypropylene in most β-type crystal polypropylene resin products is higher than 60 percent, and the notched impact strength of the above products is 1-1.5 times higher than that of the α-type crystal polypropylene from which the β-type crystal polypropylene resin is obtained. When the β-type crystal polypropylene is blended with propylene copolymers, a new type of polypropylene resin is obtained. (Paper received 15 Sep 86.)

CSO: 4009/1072

STUDY OF KINETICS OF BUTADIENE POLYMERIZATION WITH $Ni(naph)_2$-$BF_3 \cdot OEt_2$-$Al(i\text{-}Bu)_3$-$BF_3 \cdot OEt_2$ CATALYST SYSTEM--THE EFFECT OF PREMIXING OF Ni-B ON THE ACTIVITY OF CATALYST

Lanzhou HECHENG XIANGJIAO GONGYE [SYNTHETIC RUBBER INDUSTRY] in Chinese Vol 10 No 1, Jan 87 pp 13-17

[English abstract of article by Chen Dianbao [7115 3329 1405], et al., of Qingdao Institute of Chemical Technology]

[Text] The kinetic behavior of butadiene polymerization with $Ni(naph)_2$-$BF_3 \cdot OEt_2$-$Al(i\text{-}Bu)_3$-$BF_3 \cdot OEt_2$, or Ni-B-Al-B, as catalyst in hydrogenated gasoline has been studied. The effects of polymerization temperature, polymerization time and premixing of Ni-B on the rate of polymerization have been investigated. The results show that the rate of polymerization is the first order with respect to the concentration of the monomer. The total activation energy of butadiene polymerization is 51.4 kJ/mol, and the efficiency of the principal catalyst is larger than 20 percent, which increases with an increase in the polymerization temperature. (Paper received 16 Jun 86.)

REFERENCES

〔1〕 Tkáč, A. and stäckc, A., Collect. Czech. Chem.Comm., 37, 1006(1972).

〔2〕 陈滇宝、梁玉华、周治华、唐学明，合成橡胶工业，8〔5〕，323.1985)。

〔3〕 陈滇宝、吴枫.梁玉华、唐学明，合成橡胶工业、9(5)，331（1986）。

〔4〕 华士英、唐学明，高分子通讯，〔5〕,331(1982)。

〔5〕 焦书科、汪松泽等，合成橡胶工业，3〔3〕，155 (1980)。

〔6〕 倪少儒、高绪国、唐学明，高分子通讯，〔1〕，241(1983)。

〔7〕 堤谷勤，石油与石油化学(日文),13，99 (1969).

〔8〕 陈滇宝、许光、唐学明，高分子学术论文报告会预印集，B25，150(1985)。

〔9〕 唐学明、林树森、严春琛，合成橡胶工业,3〔1〕，13(1980)。

〔10〕 曹湘洪，合成橡胶工业，8〔5〕,315(1985)。

CSO: 4009/1072

STUDY OF SIMULTANEOUS INTERPENETRATING NETWORKS OF POLYBUTADIENE-BASED POLYURETHANE/POLY(STYRENE-DIVINYLBENZENE)

Lanzhou HECHENG XIANGJIAO GONGYE [SYNTHETIC RUBBER INDUSTRY] in Chinese Vol 10 No 1, Jan 87 pp 21-26

[English abstract of article by Jia Demin [6328 1795 3046], et al., of the Materials Science Research Institute, South China Institute of Technology, Guangzhou]

[Text] The IPNs of polybutadiene-based polyurethane/poly(styrene-divinylbenzene) [PU(HTPB)/P(St-DVB)-IPN] have been synthesized by simultaneous polymerization. The results of FTIR and extraction experiments show that PU(HTPB) and P(St-DVB) form interpenetrating polymer networks which contain little quantities of chemically-bonded copolymers of PU(HTPB) and P(St-DVB). TEM confirms that the IPNs exhibit a special cellular structure which, within the range of P(St-DVB content from 30-60 percent, forms the dual phase continuity. The results of DMS and DSC indicate that the interpenetration and "forced compatibility" between the hard domains of PU(HTPB) and P(St-DVB) are more obvious than between the soft segments of PU(HTPB) and P9St-DVB). The mechanical properties of the IPNs are far better than those of PU(HTPB). Under the same test conditions, the tensile strength and elongation at the PU(HTPB) break are 2.84 MPa and 600 percent respectively; whereas the tensile strength and elongation at the break of IPNs are 11.76 MPa and 800 percent respectively. (Paper received 19 May 86.)

REFERENCES

[1] Allen,G.,et al.,Polymer,15(1),13(1974).

[2] 李玉玮等,高等学校化学学报,5(1),105(1984).

[3] 山西省化工研究所编,"聚氨酯弹性体",化学工业出版社,94(1985).

[4] J.A.曼森,L.H.斯珀林编,汤华远译,"聚合物共混物及复合材料",化学工业出版社,第八章,(1983).

[5] 涂林、贾德民、王孟钟,特种橡胶制品,7(1),52(1986).

[6] Frisch, H.L.,et al., "Chemistry and Properties of Crosslinked Polymers", New York, 205(1977).

CSO: 4009/1072

EFFECT OF POLYPHENYLPHENYL-POLYVINYL SILICONE OIL ON PROPERTIES OF HEAT CURABLE HIGH STRENGTH AND HEAT RESISTANT SILICONE RUBBER

Lanzhou HECHENG XIANGJIAO GONGYE [SYNTHETIC RUBBER INDUSTRY] in Chinese Vol 10 No 1, Jan 87 pp 32-36

[English abstract of article by Feng Shengyu [7458 5110 3768], et al., of the Department of Chemistry, Shandong University, Jinan]

[Text] The effects of polyphenylphenyl-polyvinyl silicone oil on various properties of heat curable high strength and heat resistant silicone rubbers cured by a peroxide curing agent have been studied. The results show that the vulcanizates of silicone rubber extended with polyphenylphenyl-polyvinyl silicone oil exhibit fine mechanical properties and heat resistance, and the higher the added amount of polyphenylphenyl-polyvinyl silicone oil, the better the mechanical properties and heat resistance. The tear strength and tensile strength of some vulcanizates before aging can reach as high as 74.4 kN/m and 11.37 MPa, respectively. The tensile strength of some vulcanizates still remains at 5.98 MPa after aging at 280°C for 24 hours. (Paper received 12 Aug 86.)

REFERENCES

〔1〕 杜作栋、陈剑华、史保川，高分子通讯，〔3〕，174（1981）。

〔2〕 同上，〔2〕，110（1983）。

〔3〕 Johnson, John R., Org. Syn. Coll., 〔3〕, 806（1955）。

〔4〕 Freeburger, M.E., et al., J. Org. Chem., 35, 652（1970）。

〔5〕 山东大学、济南石化四厂，高强度抗撕裂硅橡胶研制技术总结，内部资料，（1975）。

9717
CSO: 4009/1072

ALGORITHM OF COMPLETE DECODING OF DOUBLE-ERROR-CORRECTING GOPPA CODES

Beijing DIANZI KEXUE XUEKAN [JOURNAL OF ELECTRONICS] in Chinese Vol 8, No 5, Sep 86 pp 321-327

[Article by Feng Guiliang [7458 6311 5328] and Xu Peihua [1776 0160 5478], Shanghai Institute of Computer Technology: "An Algorithm of Complete Decoding of Double-Error-Correcting Goppa Codes"; received 11 Dec 1984, revised draft received 11 May 1985; first paragraph is source supplied English abstract]

[Text] Abstract: In this paper an algorithm of complete decoding procedure for the Goppa codes with generator polynomial $G(z)=z^2+z+\beta$ and parameters $(2^m, 2^m-2m, 5)$ is shown. The algorithm requires at most m times calculating inner product of vectors over GF(2) and finding roots of quadratic equation in $GF(2^m)$. For $m \le 12$, the algorithm has been realized.

I. Introduction

Since very little is currently known about perfect codes, the efforts of many researchers are concentrated on quasi-perfect codes and near quasi-perfect codes[1]. As early as 1960, reference [2] pointed out that the all error-correcting primitive binary BCH codes are quasi-perfect. Complete decoding of these types of codes is given in references [3] and [4]. In 1981, reference [5] proved that when m is an odd number, binary Goppa codes which have parameters $(2^m, 2^m-2m)$ are quasi-perfect. Recently, reference [6] proved that for a given checker, only when m is an even number, and the checker $S_1=0$ line $S_3=1$, is the corresponding residual jishou [7162 7445]'s weight ≤ 3; when m is an even number, the weight of the residual jishou of the corresponding $S_1=0$ and $S_3=1$ is 4. For this reason, reference [6], in addition to proving that when m is an odd number, a double-error-correcting binary Goppa code is a quasi-perfect code, also proved that a double-error-correcting binary Goppa code when m is an even number is a near quasi-perfect code; in addition it also provided a complete decoding process. This paper focuses on the complete decoding process for double-error-correcting binary Goppa codes provides by reference [6] and gives a specific algorithm for carrying out this process. This algorithm requires only at GD(2), calculating at most m times of the inner product of m dimension vectors and finding roots of the quadratic equation in order to carry out complete decoding of the double-error-correcting binary Goppa code. For $m \le 12$, the decoding calculations in this paper were carried out on an IBM-PC computer.

II. Complete Decoding Process

This paper considers double-error-correcting binary Goppa code of parameters $(2^m, 2^m-2m, 5)$ and having generator polynomial $G(z)=z^2+z+\beta$. The complete decoding of such a Goppa code is, given any two values S_1 and S_3 at $GF(2^m)$, find the smallest positive integer t and $x_1, x_2, \ldots, x_t$ at $GF(2^m)$, establish

$$\left.\begin{aligned} \sum_{i=1}^{t} \frac{1}{x_i^2 + x_i + \beta} &= S_1, \\ \sum_{i=1}^{t} \frac{x_i}{x_i^2 + x_i + \beta} &= S_3, \end{aligned}\right\} \tag{1}$$

in which $G(z)=z^2+z+\beta$ is a irreducible polynomial at $GF92^m)$.

From reference [6] we know that if m is an odd number, then $t \leq 3$; if m is an even number, and $S_1 \neq 0$ or $S_3 \neq 1$, then $t \leq 3$; if m is an even number, and $S_1=0$ and $S_3=1$, then $t=4$. The specific decoding process is:

(1) If $S_1=0$, and $S_3=0$, then no error occurs.

(2) If $S_1 \neq 0$, and $\left(\frac{S_3}{S_1}\right)^2 + \left(\frac{S_3}{S_1}\right) + \beta = \frac{1}{S_1}$, then $t=1$, $x_1 = \frac{S_3}{S_1}$.

(3a) If $S_1 \neq 0$, $S_3=0$, and $\mathrm{tr}\left(\frac{1}{\beta S_1^2}\right) = 1$, then double error occurs. First solve for x_2 from equation (2), then solve for x_1 from equation (3).

$$(S_1 + \beta S_1^2)x_2^2 + \beta S_1^2 x_2 + \beta(S_1 + \beta S_1^2) = 0, \tag{2}$$

$$x_1 = \frac{S_3 y_2 + x_2}{S_1 y_2 + 1}, \tag{3}$$

in which $y_i = x_i^2 + x_i + \beta \ (i = 1, 2)$ and $\mathrm{tr}(\alpha) = \sum_{i=0}^{m-1} \alpha^{2^i}$.

(3b) If $S_1=0$, $S_3 \neq 0$, and $\mathrm{tr}\left(\frac{1}{S_3}\right) = 1$, then double error occurs. First solve for x_2 from equation (4), and then solve for x_1 from equation (3).

$$S_3^2 \cdot x_2^2 + S_3^2 \cdot x_2 + (S_3^2 \cdot \beta + S_3) = 0. \tag{4}$$

(4a) If $S_1 \neq 0$, $-\frac{1}{\beta}-$, $S_3=0$, and $\mathrm{tr}\left(\frac{1}{\beta S_1^2}\right) = 0$, then three errors occur. First of all, determine $\theta 0$, and $\theta 1$ from equation (5), then solve x_1 from equation (6), next solve x_2 from equation (7), and finally solve x_3 from equation (8).

$$\frac{\beta^{\frac{1}{2}} + \frac{1}{S_1^{1/2}} + \frac{1}{S_1}}{\theta_0} + \frac{\frac{1}{\beta^2 S_1^3}}{\theta_1} = 1 + \frac{1}{\beta S_1}. \tag{5}$$

in which $\mathrm{tr}(\theta_0) = 0$, $\mathrm{tr}(\theta_1) = 1$,

$$x_1^2 + \left(1 + \frac{1}{\beta S_1} + \frac{1}{\beta^2 S_1^3 \theta_1}\right) x_1 + \left(\beta + \frac{1}{\beta S_1^2} + \frac{1}{\beta^2 S_1^4 \theta_1}\right) = 0, \tag{6}$$

$$(p + y_1 S_1) x_2^2 + (1 + p) x_2 + p\left(\beta + \frac{1}{S_1}\right) = 0, \tag{7}$$

in which $p = y_1 \cdot \beta \cdot S_1^2 + S_1 \cdot x_1$,

$$x_3 = \left(S_3 + \frac{x_1}{y_1} + \frac{x_2}{y_2}\right) \Big/ \left(S_1 + \frac{1}{y_1} + \frac{1}{y_2}\right). \tag{8}$$

(4b) If $S_1=0$, $S_3 \neq 0$, 1, and $\mathrm{tr}\left(\frac{1}{S_3}\right) = 0$, then three errors occur. First of all determine θ_1, and θ_2 from equation (9), then solve x_1 from equation (10), next solve x_2 from equation (11), and finally solve x_3 from equation (8).

$$\frac{1 + S_3}{S_3^4} = \theta_1 \cdot \theta_2. \tag{9}$$

in which $\mathrm{tr}(\theta_1) = \mathrm{tr}(\theta_2) = 1$,

$$x_1^2 + x_1 + \left(\beta + \frac{1}{S_3} + \frac{1}{S_3^2} + \frac{1 + S_3}{S_3^4 \theta_1}\right) = 0, \tag{10}$$

$$x_2^2 \left(1 + \frac{1}{q S_3^2}\right) x_2 + \left(\beta + \frac{1}{S_3} + \frac{1 + x_1}{q S_3^2}\right) = 0, \tag{11}$$

in which $q = y_1 + \frac{1}{S_3}$.

(5) If $S_1=0$, $S_3=1$, and m is an even number, then four errors will occur. first of all determine u and v, so that $\frac{1}{u} + \frac{1}{v} = 1$ and $\mathrm{tr}(u)=\mathrm{tr}(v)=1$ are established. Then from equation (12) solve x_1 and x_2, and finally x_3 and x_4 from equation (13).

$$x_1^2 + x_1 + \beta = x_2^2 + x_2 + \beta = u, \tag{12}$$

$$x_3^2 + x_3 + \beta = x_4^2 + x_4 + \beta = v. \tag{13}$$

In the above complete decoding process, except for equations (5) and (9), the other equations all are binomial equations on $GF(2^m)$. Reference [7] provided the formula for finding roots of binomial equations, and naturally we can also find binomial roots through solving the m linear equation group at GF(2). For this reason, the key to the above complete decoding process is how to find the roots of equations (5) and (9). In the third section we will give the algorithm for finding the roots of equations (5) and (9). This algorithm at most requires calculating the inner product of the m dimension vectors at GF(2) m times.

III. Finding Roots in Equations (5) and (9)

Supposing $r, r^2, \ldots, r^{2m-1}$ is a group of standard bases at $GF(2^m)$ (reference [1], p. 122, theorem 25), then any element X in $GF(2^m)$ can be written $X = x_0 r + x_1 r^2 + \ldots + x_{m-1} \cdot r^{2m-1}$, and recorded as $X \underline{\underline{\Delta}} (x_0, x_1, \ldots, x_{m-1})$, in which $x_j \varepsilon GF(2)$. Let $A = (a_0, a_1, \ldots, a_{m-1})$, $a_j \varepsilon GF(2)$ is easily known.

$$\mathrm{tr}(A \cdot X) = \sum_{j=0}^{m-1} f_j(x_0, x_1, \cdots, x_{m-1}) \cdot a_j, \tag{14}$$

in which $f_j(x_0, x_1, \cdots, x_{m-1}) = \sum_{i=0}^{m-1} f_j^{(i)} \cdot x_i$ and $f_j^{(i)} \in GF(2)$.

Written

$$F = \begin{bmatrix} f_0^{(0)} & f_0^{(1)} \cdots f_0^{(m-1)} \\ f_1^{(0)} & f_1^{(1)} \cdots f_1^{(m-1)} \\ \vdots & \vdots \quad\quad \vdots \\ f_{m-1}^{(0)} & f_{m-1}^{(1)} \cdots f_{m-1}^{(m-1)} \end{bmatrix}.$$

Lemma 1 F is a nonsingular array, i.e., $\det F \neq 0$.

Proof Use the proof by contradiction. If $\det F = 0$, then its m series linearity correlates (on GF(2)), i.e., there is not complete zero $C_0, C_1, \ldots, C_{m-1} \varepsilon GF(2)$ so that

$$F \cdot \begin{bmatrix} C_0 \\ C_1 \\ \vdots \\ C_{m-1} \end{bmatrix} = \begin{bmatrix} 0 \\ 0 \\ \vdots \\ 0 \end{bmatrix}$$

is established. Written $C=(C_0, C_1, \cdots, C_{m-1}) \in GF(2^m)$. From Eq. (14) we know

$$\begin{bmatrix} \mathrm{tr}(Cr) \\ \mathrm{tr}(Cr^2) \\ \vdots \\ \mathrm{tr}(Cr^{2^{m-1}}) \end{bmatrix} = \begin{bmatrix} 1 & 0 & 0 \cdots 0 \\ 0 & 1 & 0 \cdots 0 \\ \vdots & \vdots & \vdots \quad \vdots \\ 0 & 0 & 0 \cdots 1 \end{bmatrix} F \begin{bmatrix} C_0 \\ C_1 \\ \vdots \\ C_{m-1} \end{bmatrix} = \begin{bmatrix} 0 \\ 0 \\ \vdots \\ 0 \end{bmatrix}.$$

For this reason, any element $A \in GF(2^m)$,

$$\mathrm{tr}(C \cdot A) = \mathrm{tr}\left(\sum_{j=0}^{m-1} a_j \cdot C \cdot r^{2^j}\right) = \sum_{j=0}^{m-1} a_j \mathrm{tr}(C \cdot r^{2^j}) = 0.$$

However, C=0. This is impossible. (QED)

Lemma 2 There are m elements $Y_1, Y_2, \cdots, Y_m \in GF(2^m)$, their trace $\mathrm{tr}(Y_i)=1(i=1, 2, \cdots, m)$ causes $\det Y \neq 0$, in which $Y_i^{-1}=(Y_{0i}, Y_{1i}, \cdots, Y_{m-1,i})$.

And

$$Y = \begin{bmatrix} y_{01} & y_{11} \cdots y_{m-1,1} \\ y_{02} & y_{12} \cdots y_{m-1,2} \\ \vdots & \vdots \quad\quad \vdots \\ y_{0m} & y_{1m} \cdots y_{m-1,m} \end{bmatrix}.$$

Proof Also uses the proof by contradiction. Supposing $Y_1, Y_2, \ldots, Y_p$ is all the elements with trace 1 in $GF(2^m)$, here p is the number of all elements with trace 1 in $GF(2^m)$. Again written

$$D = \begin{bmatrix} y_{01} & y_{11} \cdots y_{m-1,1} \\ y_{02} & y_{12} \cdots y_{m-1,2} \\ \vdots & \vdots \\ y_{0p} & y_{1p} \cdots y_{m-1,p} \end{bmatrix},$$

in which $Y_i^{-1}=(y_{0i}, y_{1i}, \cdots, y_{m-1,i})$, $y_{ij} \in GF(2)$.

If there are not such m elements which cause lemma 2 to be established, then the order of $D \leq m-1$, therefore there cannot be completely zero $C_0^*, C_1^*, \cdots, C_{m-1}^*$, $C_i^* \in GF(2)$, so that

$$D \cdot \begin{bmatrix} C_0^* \\ C_1^* \\ \vdots \\ C_{m-1}^* \end{bmatrix} = \begin{bmatrix} 0 \\ 0 \\ \vdots \\ 0 \end{bmatrix} \quad (15)$$

is established. Also, known from Lemma 1. There must be $C_0, C_1, \cdots, C_{m-1}$, $C_i \in GF(2)$, which are not completely zero, so that

$$F \cdot \begin{bmatrix} C_0 \\ C_1 \\ \vdots \\ C_{m-1} \end{bmatrix} = \begin{bmatrix} C_0^* \\ C_1^* \\ \vdots \\ C_{m-1}^* \end{bmatrix} \qquad (15')$$

is established. Synthesizing Eqs (15) and (15'), and using the notation of Eq. (14) we know: $\mathrm{tr}(C \cdot Y_j^{-1}) = 0 (j = 1, 2, \cdots, p)$,

in which $C = (C_0, C_1, \cdots, C_{m-1}) \neq 0$. Let $Z_j = C \cdot Y_j^{-1}$,

then $\mathrm{tr}(Z_j)=\emptyset$. From this, when Y_j (qubian [0648 6664]) all elements whose trace is 1, all have Z_j whose trace is zero. Therefore, C cannot be divided into $\theta_1 . \theta_2$, in which $\mathrm{tr}(\theta)=\mathrm{tr}(\theta_2)=1$. This is in contradiction with Theorem 3 of reference [6]. (QED)

Theorem 1 For any given A=0, there must be a $Y_j (1 \leqslant j \leqslant m)$, so that $\mathrm{tr}\ (A.Y^{-1})=1$ is established. That is, for the equation $A=\theta_1, \theta_2, \mathrm{tr}(\theta_1)= \mathrm{tr}(\theta_2)=1$, there must be a Y_j which is one of its solutions in which $1 \leqslant \ j \leqslant m$.

Proof From the above notation we know

$$\begin{bmatrix} \mathrm{tr}(A \cdot Y_1^{-1}) \\ \mathrm{tr}(A \cdot Y_2^{-1}) \\ \vdots \\ \mathrm{tr}(A \cdot Y_m^{-1}) \end{bmatrix} = Y \cdot F \cdot \begin{bmatrix} a_0 \\ a_1 \\ \vdots \\ a_{m-1} \end{bmatrix}.$$

Because $A \neq 0$, therefore, not all $a_0, a_1, \ldots, a_{m-1}$ are zero. Also, from Theorem 1 and Lemma 2 we know that Y . F is non singular, therefore not all $\mathrm{tr}(A Y_j^{-1}) (j = 1, 2, \cdots, m)$ is zero. Thus, at least there is a $j (1 \leqslant j \leqslant m)$, which establishes $\mathrm{tr}(A \cdot Y_j^{-1}) = 1$

(QED)

Notation $Y^*=Y \cdot F$. From Theorem 1 it is very easy to obtain algorithm 1 of a solution to Equation (9).

Algorithm 1 Given S_3, let $A = \frac{1 + S_3}{S_3^3} \triangleq (a_0, a_1, \cdots, a_{m-1}) \neq 0$,

successively carry out the inner product of matrix Y^* line $(y_{0j}^*, y_{1j}^*, \cdots y_{m-1j}^*)$

If the inner product of the jth line is 1, then Y_j is a solution of Equation (9).

This is because Y^* only has m lines. Again from Theorem 1 we know that at most carrying out calculation of the inner product of the m dimension vector at GF(2) m times we can obtain a solution of Equation (9).

Below we discuss the problem of finding a solution to Equation (5). Let

$A^* = (a_0^*, a_1^*, \cdots, a_{m-1}^*)$ satisfies

$$\begin{bmatrix} 1 \\ 1 \\ \vdots \\ 1 \end{bmatrix} = Y^* \begin{bmatrix} a_0^* \\ a_1^* \\ \vdots \\ a_{m-1}^* \end{bmatrix}. \tag{16}$$

Lemma 3 If A≠A*, then there must be a $Y_j (1 \leqslant j \leqslant m)$ so that

$$\mathrm{tr}(A \cdot Y_j^{-1}) = 0.$$

Proof Using the proof by contradiction. If for each $j (1 \leqslant j \leqslant m)$, there is $\mathrm{tr}(A.y^{-1})=1$, then

$$\begin{bmatrix} 1 \\ 1 \\ \vdots \\ 1 \end{bmatrix} = Y^* \begin{bmatrix} a_0 \\ a_1 \\ \vdots \\ a_{m-1} \end{bmatrix}. \tag{17}$$

Comparing Eq. (16) and Eq. (17), then from the non-singularity of matrix Y* we know that A=A* and this contradicts the conditions already known. (QED)

For each m there are only two possible situations:

(1) There is a $\tilde{\theta}_0$ and a $\tilde{\theta}_1$, in which $\mathrm{tr}(\tilde{\theta}_0) = 0$, $\mathrm{tr}(\tilde{\theta}_1) = 1$,
thus $A^* = \tilde{\theta}_0 \cdot \tilde{\theta}_1$

(2) There is not a θ_0 and θ_1, in which $\mathrm{tr}(\theta_0) = 0$, $\mathrm{tr}(\theta_1) = 1$,
thus $A^* = \theta_0 \cdot \theta_1$

For the equation

$$A = \theta_0 \cdot \theta_1, \tag{18}$$

in which $\mathrm{tr}(\theta_0)=0_1 \mathrm{tr}(\theta_1)=1$ we have:

Algorithm 2 If A≠A*, calculate its successively with the inner product of matrix Y*, and if the inner product of A and Y_j^*, then Y_j is a solution of Equation (18).

If A=A*, and if m satisfies condition (1), then $\tilde{\theta}_0$, $\tilde{\theta}_1$ are a solution of Equation (18); otherwise, equation (18) has no solution.

Now we will consider Equation (5), it is equivalent to

$$\frac{\dfrac{\beta^{1/2} \cdot S_1 + S_1^{1/3} + 1}{S_1} \cdot \dfrac{\beta S_1}{\beta S_1 + 1}}{\theta_0} + \frac{\dfrac{1}{\beta^2 \cdot S_1^3} \cdot \dfrac{\beta S_1}{\beta S_1 + 1}}{\theta_1} = 1. \tag{19}$$

let
$$A' = \frac{\beta^{1/2} \cdot S_1 + S_1^{1/2} + 1}{S_1} \cdot \frac{\beta S_1}{\beta S_1 + 1} = \beta^{1/2} + \frac{\beta}{1 + \beta S_1} + \frac{\beta^{1/2}}{1 + \beta^{1/2} \cdot S_1^{1/2}}$$

and
$$B' = \frac{1}{\beta S_1^2 (1 + \beta S_1)},$$

then
$$\mathrm{tr}(A') = \mathrm{tr}(\beta^{1/2}) = 1. \tag{20}$$

Now equation (19) becomes
$$\frac{A'}{\theta_0} + \frac{B'}{\theta_1} = 1, \tag{21}$$

i.e.,
$$\theta_1 = B' + \frac{A' \cdot B'}{A' + \theta_0}. \tag{22}$$

Again, supposing $A=A'.B'$, because $\mathrm{tr}(\theta)=1$, therefore Equation 22) becomes $\mathrm{tr}(B^1 + \frac{A}{\theta_1^*}) = 1$, in which $\theta_1^* = A + \theta_0$. If $\mathrm{tr}(B')=0$, then $\mathrm{tr}(\frac{A}{\theta_1^*}) = 1$. We can use algorithm 1 to find θ_j^*, then we can find θ_0 and θ_1; if $\mathrm{tr}\,(B')=1$, then $(\frac{A}{\theta_1^*})=0$ because Equation (5) must have a solution, therefore we can use algorithm 2 to find θ_1^* and then solve θ_0 and θ_1.

From the above discussion we know that from at most m times calculating the m vector inner product at GF(2), we can always find a solution of Equation (5) and Equation (9).

IV. Examples

Example 1 For the situation m=5, supposing α is an original element of $GF(2^5)$ and $\alpha^5+\alpha+1=0$. We can assume $Y_1 = \alpha^{11}$, $Y_2 = \alpha^{22}$, $Y_3 = \alpha^{13}$, $Y_4 = \alpha^{26}$ and $Y_5 = \alpha^{21}$. By Algorithm 1, for any non-zero element in $GF^*(2^5)$, there must be $Y_j (1 \leqslant j \leqslant 5)$, which satisfies Equation (9).

For example, assuming $A = \alpha^{14}$, from Algorithm 1 it is readily known that $\theta_1 = \alpha^{11}$, $\theta_2 = \alpha^3$ satisfying $A=\theta_1 \cdot \theta_2$, and $\mathrm{tr}(\theta_1)=\mathrm{tr}(\theta_2)=1$.

Example 2 For the situation m=4, supposing α is an original element of $GF(2^4)$, and $\alpha^4 + \alpha + 1 = 0$. We can assume $Y_1 = \alpha^7$, $Y_2 = \alpha^{14}$, $Y_3 = \alpha^{13}$ and $Y_4 = \alpha^{11}$.

Thus A*=1. By Algorithm 2, for any A($a \neq 0,1$) in GF(2^4), there is always a $Y_j (1 \leq j \leq 4)$ which is a solution of Equation (18). And for A=1, it is easy to prove that $\theta_1=\alpha^4$ and $\theta_0=\alpha^4$ is a solution to Equation (18).

For example, $\frac{\alpha^3}{\theta_0} + \frac{\alpha^6}{\theta_1} = \alpha^{12}$, i.e., $\frac{\alpha^6}{\theta_0} + \frac{\alpha^9}{\theta_1} = 1$.

Under these circumstances, $A=\alpha^6 . \alpha^9=1$. For Algorithm 2 we know that $\theta_1^*=\alpha^{11}$, and from $\theta_1^*=A'+\theta_0$ we know $\theta_0=\alpha$. Thus $\theta_0=\alpha$ and $\theta_1=\alpha^{14}$ are solutions to

$\frac{\alpha^3}{\theta_0}+\frac{\alpha^0}{\theta_1}=\alpha^{12}$ in which $tr(\theta_0)=0$, $tr(\theta_1)=1$.

REFERENCES

[1] F.J. Macwilliams and N.J.A. Sloane, "The Theory of Error-Correcting Codes," North-Holland, 1977.

[2] D.C. Gorenstein, W.W. Peterson and N. Zierler, INFOR. AND CONTROL, 3(1960), 291-4.

[3] C.R.P. Hartmann, IEEE TRANS. ON IT, IT-17 (1971), 765-6.

[4] Feng Guiliang [7458 6311 5328], DIANZI KEXUE XUEKAN, 5(1983), 343-8.

[5] O. Moreno, "Goppa Codes Related Quasi-perfect Double-error-correcting Goppa Codes," Presented at IEEE Int. Symposium on Information Theory, Santa Monica, U.S.A., 1981.

[6] G.L. Feng and K.K. Tseng, "On Quasi-perfect Property of Double-error-correcting Goppa Codes and Their Complete Decoding," Presented at IEEE Int. Symposium on Information Theory, St. Jovite, Quebec, Canada, 1983.

[7] C.L. Chen, IEEE TRANS. ON IT, IT-28 (197=82), 792-4.

8226/7358
CSO: 4008/1037

COASTAL FOREST BELT SUGGESTED FOR ECOLOGICAL REASONS

OW121352 Beijing XINHUA in English 1325 GMT 12 Mar 87

[Text] Beijing, 12 Mar (XINHUA)--China should build a 4.8-million-hectare coastal forest belt in the next 14 years to improve coastal ecological conditions, the vice-minister of forestry proposed today.

Vice-minister Liu Guangyun suggested, "By 1995, China should plant 4.35 million hectares of barren hills and coastal land with trees, foliate 370,000 hectares of saline-alkali soil with shrubs and grass, and form an agricultural-forest network involving 160,000 hectares."

"Trees and foliage are needed as protection against water, wind and sand, and for soil and water conservation," Liu said, adding by the year 2000, forest coverage could increase from the current 19 to 38 percent.

"The proposed coastal afforestation project would aid further development of the country's coastal areas now open to the outside world," Liu said, "and the coastal belt would be another afforestation project following the lead of the six-million-hectare shelter-belt in northern China."

China's 18,000-kilometer coast line includes 180 counties, and the area started building coastal shelter-belts in the 1950s to combat wind, sand, drought, flood and typhoons, which strike the area an average of 9 tims a year.

"The original project was not well-planned, so typhoons and other disasters often disrupted the area's people and economy," Liu said.

"To accelerate coastal shelter-belt construction," Liu said, "It is necessary to set up and improve a responsibility system in afforestation, and compensate people living in coastal areas for their work."

"Policies should be more flexible," Liu stressed, "and the Army could plant coastal areas and islands on contract if the local population is in no position to do so." Liu also encouraged inland surplus manpower to contract for afforestation projects with the people living along the coast or on the islands.

According to Liu, China is also seeking overseas donations or investment to help with the country's afforestation projects.

/6662
CSO: 4010/2011

BIOGRAPHIC INFORMATION ON 19 NOTED S&T PERSONALITIES

Beijing KEJI RIBAO in Chinese 14 Jan 87 p 2

[Text] Zhou Jihu, S&T Entrepreneur

Zhou Jihu [0719 1015 3275], 26, high school graduate, who after failing his college entrance exams, began an arduous, tortuous course of self-study. He brought wealth to his neighborhood, and invested 50,000 yuan to start the Wuchang County Civilian Institute of Special Local Produce Cultivation. The institute has focused on raising Buthus martensi and has also disseminated two "spark plan" projects of Actinidia chinensis and the high level nutrition product Amorphophallus rivieri. Last year, he was employed by the Institute of Comprehensive Technology of Wuhan University as an assistant researcher.

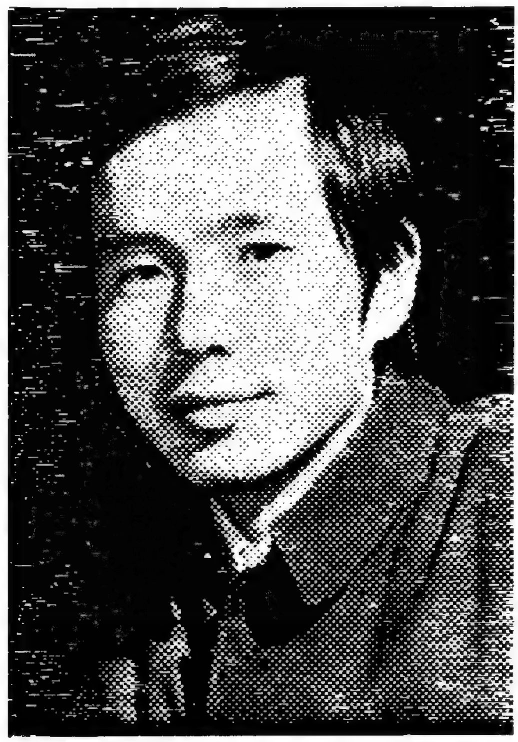

Cheng Baoquan, New Star in Economics

Cheng Baoquan [4453 2128 0356], 26, a new star in the field of economic theory in this country. When he was 21, he wrote "Qualitative Economics" in some 1 million words, which was recommended for publication by Comrade Sun Yefang [1327 0396 2455] and which has made pioneering contributions to qualitative economic theory. In 1984, Chapter 4, "On Using 10 Simple Mathematical Calculations to Check the Economic Nature of Enterprise Quality," was included among the top level of published papers at the World Scholastic Conference on Quality. He is currently deputy chairman of the economics commission of Huangguang Prefecture in Hubei.

Hu Xihua, Designer of the Tianjin Butterfly Lijiao Bridge

Hu Xihua [5170 5045 5478], 30, technical school graduate, designer of the butterfly Lijiao Bridge at the Zhongshan Gate in Tianjin. Because of the novel shape of the Lijiao Bridge, its complete functionality, compact design, little to demolish and remove, and that it was also economical, it was well received by leaders and specialists at all levels. Recently, the city of Tianjin broke rules to promote him to be an engineer at the Tianjin Municipal Academy of Engineering Survey and Design.

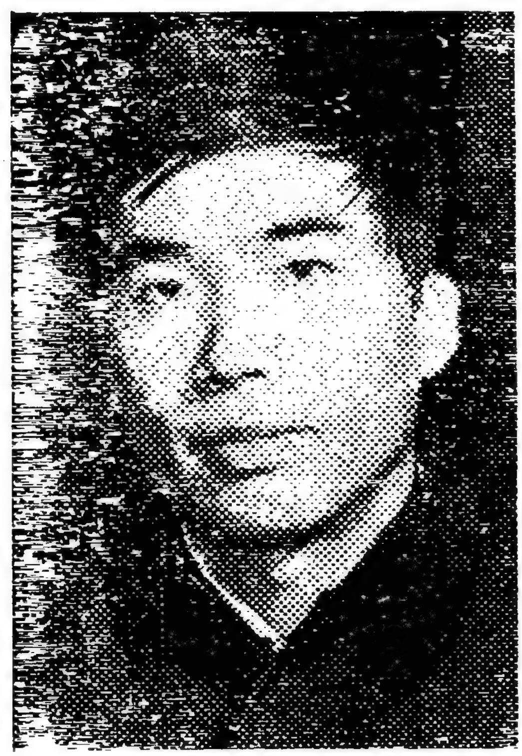

Zheng Weian, College Professor Who Started As a Carpenter

Zheng Weian [6774 0251 1344], 34, started as a carpenter, never attended college, but through self-study exhibited his talent in mathematics. In 1978, he qualified by examination for the Huadong Normal Graduate Academy, and after receiving a masters degree went to France for advanced studies, where he received a French national doctorate. He has published more than 20 high quality academic papers, among which some of his insights into differential manifold studies have been called "Mr. Zheng's Theorem" by French mathematics authorities, and this mathematic derivation process has been called the "Zheng process." In January 1986, he was promoted more than one grade at a time to be a professor in the mathematics and statistics department of the Huadong Teacher's College and an adviser to PhD students.

Ma Li, A Factory Director Who Understands Technology and Is Good at Operations

Ma Li [7456 0500], 39, Hui nationality, factory director of the Wuzhong City, Ningxia, collective enterprise Plastics Weaving Plant. After graduation from high school, he entered the plant as an apprentice, and is now an expert who understands technology and is good at operations management. The plant that he directs formerly was a small plant on the brink of bankruptcy that had developed into a modern, "dual culture" large-scale enterprise. It is one of the best in the country for the assimilation and application of imported production lines for plastic woven bags and for having the highest level of management. Its production volumes are at the forefront of 700 firms in the same business throughout the country.

Li Zhongqi, Number One in "Fireworks"

Li Zhongqi [7812 0112 3971], 41, high school graduate, technician at the Liuyang Export Fireworks Plant in Hunan. In 1986, he took the first place in the 21st International Fireworks Competition in Monaco, and he won a gold cup among similar products in the national Hundred Flowers award evaluation competition. Over the last 10 and more years, he has picked up specialized knowledge on his own, has taken charge of science research projects, and has won more than 10 major science achievement awards. He has developed more than 40 new fireworks products, and since 1985 has also developed 43 new products for fireworks displays, which have made great contributions to the generation of foreign exchange by products in light industry in this country.

Wang Ming, Matured Through Self-Study

Wang Ming [3769 6900], 41, high school graduate, and currently director of the Shaanxi Province Ningqiang County Tianma Institute. Over the past 20 years, he studied botany on his own, diligently studying the technology to artificially cultivate Gastrodia elata. He has altered old methods of cultivation and invented the "cold bed seeding method for symbiotic germinating fungus," which he has disseminated throughout Ningqiang County. In only 13 years, the accumulated output for artificial cultivation of tianma is 4.7 million jin, for a value of more than 15 million yuan. For this reason, he was awarded a national science conference medal, a first prize for scientific and technical achievements in Shaanxi Province, and a first prize for national inventions.

Yao Jinzhong, Expert at Technical Innovation

Yao Jinzhong [1202 6930 6988], 48, a self-taught specialist in ultrasonic detector instrumentation design and creation, and currently the institute director of the Guangdong Province Shantou Institute of Ultrasonic Instrumentation and a high level engineer. Since 1960, he has been fighting at the first line of research, maintaining an integration of theory with practice and an integration of scientific research with production. He has paid attention to economic results, has designed and made nearly 20 new products, winning national and provincial level prizes on more than 10 occasions. The All-China Federation of Trade Unions once honored him with the title "expert at technical innovation."

Zhao Caidu, Skilled Craftsman who Works Wonders

Zhao Caidu [6392 2088 1653], 48, high school graduate, currently an assistant engineer at the Shanghai Xianfeng Electrical Machinery Plant. In the general design tasking for the key part in the key national research project "Beijing electron-positron collider" 70B bent conversion magnet mold, he overcame numerous difficulties. After great effort and strict testing, he finally completed the mission before the national holiday in 1984, having worked wonders--the mold tolerance was at the level of microns. Presently, throughout the world only the U.S. Moore Company, with its most advanced equipment, can attain this degree.

Chen Chuangtian, Specialist in Non-Linear Materials

Chen Chuangtian [7115 0482 1131], 49, researcher at the Fujian Institute on the Structure of Matter, of the Chinese Academy of Sciences. He won a 1985 prize from the National Science Meeting in major scientific and technical achievements for his research on the structure and properties of non-linear optical materials; he won a second prize from the Chinese Academy of Sciences for scientific and technical achievements for the gene modeling and new material explorations regarding non-linear optical materials. The new non-linear sodium metaborate developed under his direction won a 1986 special prize from the Chinese Academy of Sciences, and has had outstanding economic results, attracting attention and interest both in this country and abroad.

Liu Ximing, Urban Telephone Communications

Liu Ximing [0491 6932 2494], 49, assistant senior engineer at Institute No 1 of the Ministry of Posts and Telecommunications. He has made great contributions to the development of electronic exchange technology development and application and in hastening the cause of urban telephone communications in this country. In recent years, he has helped Fujian to import the first programmable digital exchange, has actively absorbed and assimilated advanced technology from abroad, and has made great contributions to developing nationally produced machinery. He directed the successful development of the first D_S--2000 programmed digital telephone exchange in this country, which attained a level equal to that internationally in the early 1980s.

Lei Yonghe, "King of Tobacco"

Lei Yonghe [7191 3057 0735], 51, called the "King of Tobacco" for long service and support of the cultivation technology and improved varieties selection for flue-cured tobacco in Yunnan. The two tobacco varieties he selected, the "Red Flower Gold Dollar" and the "Sipeite G-28", have been disseminated throughout 95 percent of flue-cured tobacco growing fields, and of which the Sipeite-28 has been disseminated and cultivated for 5 years, and economic results from which have totalled more than 70 million yuan. Five of his achievements have been awarded provincial-level and above science research achievement prizes. He is currently deputy director of the Tobacco Institute of the Yunnan Province Academy of Agricultural Sciences.

Guo Jingkun, Specialist in Inorganic Nonmetallic Materials

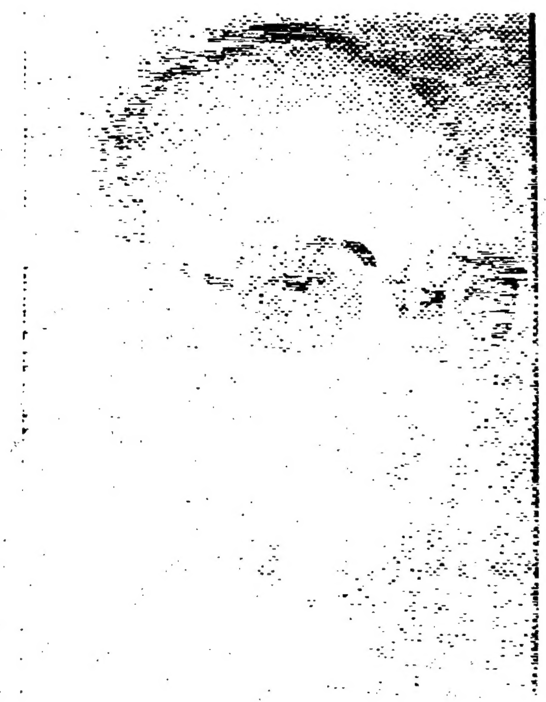

Guo Jingkun [6753 2529 0981], 53, specialist in inorganic nonmetallic materials, currently director of and assistant researcher at the Shanghai Silicate Institute of the Chinese Academy of Sciences. His research achievement "Two Kinds of High-Alundum Ceramics and Their Metallization and Sealing-in" won a national second prize for inventions; "Preparation Techniques for Carbon-Fiber Reinforced Quartz Composite" won a 1981 national first prize for inventions, and has made an outstanding contributions to economic construction in this country and to the development of sophisticated national defense technologies.

Lu Zai, Ship Engineer

Lu Zai [4151 0961], 53, senior engineer, currently senior technician at the Shanghai Jiangnan Shipyard. On several occasions, she has been responsible for work on hull design techniques, and she has participated in the technological designs for 10,000-ton steamers. The "Xiangyang Hong No 10" steamer for which she directed the design won a special prize for national scientific and technical advancement. She also contributed to recent construction of a 65,000-ton oil tanker. She is the People's Congress representative from the Luwan District of Shanghai Municipality, and is an International Working Women red-banner pacesetter for Shanghai Municipality and the Shanghai Navigation Industry Company.

Yang Puchen, Research in Special Fibers

Yang Puchen [2799 3302 5256], 54, assistant professor at the Tianjin Textile Industrial Academy and a Tianjin model worker. He has been engaged for several years in research with special fibers, and has been responsible for eight research projects as commissioned by the state and by Tianjin, among which two were awarded second prizes by the city of Tianjin for outstanding achievements in science and technology, and one won a third prize for national scientific and technical advancement, as well as an achievement award from the Ministry of the Textile Industry for science and technology problem solving. The institute of which he is a leader is one of the most important research bodies in the field of membrane disassociation research in this country. He has also taken responsibility for three major tasks in science and technology problem solving projects during the Seventh 5-Year Plan.

Li Qingwen, A Leader in Science and Technology Poverty Relief

Li Qingwen [2621 1987 2429], 55, senior agricultural technician, and director of the Liaoning Province Academy of Agricultural Sciences Institute of Cultivation. In 1982 he was commissioned by Liaoning Province to lead a brigade to the Fuxin Mongol Autonomous County to take part in the establishment of a comprehensive science experimental county for agricultural modernization. He proceeded from the actual situation of the area, restructured the cultivation system, which caused the grain output for that county in 1985 to increase by 140 million jin, by 250 million jin in 1986, and also helped farm households to set up a courtyard economy. In addition, they set up a "plant less, and produce more, with better results" cultivation system, which created a new alternative by which to restructure the cultivation system for windy arid regions.

Zhen Yongsu, Anti-Tumor Biological Missile Researcher

Zhen Yongsu [3914 3057 5685], 55, researcher. In seeking new antibiotics, he established a screening model for anti-tumor medicines. He has also had outstanding achievements in the field of applications for anti-tumor medicine pharmacology research and pathology methods in pharmacological research. He has also provided three new medicines for clinics: Guanghui toxin, Zhengguang toxin, and Pingyang toxin. First of all, he proposed using a combination of monoclonal antibodies with the Zhengguang toxin A^6 and the Pingyang toxin to develop a biological missile for tumors, and he actually obtained anti-liver cancer and stomach and throat cancer monoclonal antibodies.

Li Zhensheng, Wheat Breeding Specialist

Li Zhensheng [2621 2182 5116], 55, researcher, director of Shaanxi Province Academy of Sciences. He has been engaged in the distant hybridization and cultivation of wheat and Yanmaicao [0249 7796 5430], as well as study of the laws of genetics, for 30 years, and had made important contributions in genetic theory and in exploration of new methods for wheat cultivation. The three new varieties of Xiaoyan [1420 0249] No 4, No 5, and No 6 that he successfully cultivated were awarded a national first prize for invention. During the 5 years 1981-1985, he disseminated and cultivated a total of 24 million mu, increasing output of wheat by more than 1.2 billion jin, which amounts to more than 200 million yuan, and which won a 1986 Shaanxi Province special honorable mention award.

Zhu Senyuan, Specialist in Liquid-Fuel Rocket Engines

Zhu Senyuan [2612 2773 0337], 56, high level engineer at the First Research Institute of the Ministry of Astronautics. Long engaged in the research into new types of oxyhydrogen engines, he proposed the theory of oxyhydrogen systems and plans for implementation, resolving the problem of heat insulation in engines. He participated in the resolution of the fire reduction problem in the system test vehicle. He participated in the development and flight testing for first and second launches of the "Long March 3," and contributed to the success of our satellite launch program.

12586
CSO: 4008/2052

END